CHAPTER IV

RESULTS AND DISCUSSION

1. The preparation of beclomethasone dipropionate hydrate form

Preparation of hydrated beclomethasone dipropionate in three different sizes was controlled by adding distilled water at the rates of 7, 23, 60, 120 and 300 ml/hr with constant stirring rate of 600 rpm at 25 ± 1 °C using infusion pump. The particle sizes as revealed from laser particle size analyzer are shown in Table 3, with their respective size distribution profile curves in Appendix B.

Table 3. The average particle size of hydrated beclomethasone dipropionate crystallized at various rates of adding water (n = 3)

Rate of water addition (ml/hr)	d(v,0.1) (SD) μm	d(v,0.5) (SD) μm	d(v,0.9) (SD) μm	appearance
7	127.25 (5.09)	431.07 (14.82)	753.74 (61.13)	transparent crystals
23	85.36 (4.21)	261.67 (7.15)	694.84 (27.82)	transparent crystals
60	65.36 (3.58)	208.30 (11.75)	474.83 (46.36)	needle-like, white and bulky crystal
120	39.12 (4.07)	159.07 (17.68)	570.26 (49.17)	needle-like, white and bulky crystal
300	10.69 (0.26)	64.98 (0.73)	249.79 (3.76)	needle-like, white and bulky crystal

Note: d(v,0.1) – 10% of the distribution is below this value
d(v,0.5) – 50% of the median volume distribution is below this value
d(v,0.9) – 90% of the distribution is below this value

Crystals of the same appearance appeared when the rates of adding water were 7 and 23 ml/hr. At higher rates, crystallization resulted in white, needle-like and bulky materials. This could be explained by the three basic steps of crystallization from solution, i.e., induction of supersaturation, formation of nuclei and the growth of crystals (Rodriguez-Hornedo, 1990). In this case, the rate of water addition higher than 23 ml/hr induced the formation of nuclei at very high rate, resulting in thin, white and bulky crystals. Since the rate of nucleation became more rapid than the rate of crystal growth, the deposition on the faces of crystal was hindered, causing the crystal to become thin and bulky.

Using paddle blade, agitation destroyed concentration gradients causing homogeneity of the solution that caused the regular growth of crystals and a narrow size distribution. Unimodal and polymodal dispersion of crystals when water additions were 7 and 23 ml/hr are demonstrated in Appendix B (Figures 36 and 37 show unimodal dispersion with stirring while Figures 41 and 42 show polymodal dispersion without stirring). The preliminary study of solubility profiles of beclomethasone dipropionate at various ratios between absolute ethanol and water were characterized by a plateau of solubility curve at 25 °C, as shown in Appendix C. From the solubility profile, it indicated that when adding water to the solution of beclomethasone dipropionate in ethanol, the solubility of the compound decreased until the solution was supersaturated and suitable to produce nuclei.

Although crystallization finally results in stable form of solid particles, metastable phase may also be formed during the growth of some nuclei. This metastable phase, however, dissolved and resulted in supersaturation for the continuing growth of stable phase until the transformation was completed (Rodriguez-Hornedo, 1990). Moreover, solubility profile indicated that when the percentage of

alcohol in the solution was lower than 50, solubility of beclomethasone dipropionate approached zero resulting in an almost complete crystallization. This was the reason for maintaining 35 ml of ethanol and adding the water of 50 ml to promote condition of crystallization in this study.

By determining the median size distributions d(v,0.5) of crystals produced at the water addition rate of 7 and 23 ml/hr (Table 3), the two crystals seemed to have different size distribution when the rate of water additions were slow (7 ml/min having the largest median size). However, their d(v,0.1)and d(v,0.9) were in the same range as shown in distribution profiles in Appendix B (Figures 36 and 37). Higher median size crystals produced with water addition rate of 7 ml/hr were chosen for further studies.

These crystals obtained from water addition rate of 7ml/hr were ground with glass mortar and pestle. Ground sample was resuspended in deionized water for 72 hrs to ensure crystallinity. Since ground samples become unstable or partly amorphous after grinding, resuspension of the sample will correct unstability of crystals and this was in accordance with the method of Takahashi et al. (1984). Crystals of different sizes were separated by passing through a series of analytical sieves with apertures of 38, 75 and 150 μm. As a result, three groups of hydrated beclomethasone dipropionate crystals were obtained, i.e. crystals of sizes smaller than 38 μm, those with sizes between 38-75 μm and those with sizes between 75-150 μm. Due to very small amount of size less than 38 μm-particles obtained, they were discarded and the other two sizes along with the unground (intact) with approximately median size of 430 μm crystals were utilized for further studies.

Table 4. The particle sizes of three difference sizes of hydrated beclomethasone dipropionate

Samples	d(v,0.1) (SD) μm	d(v,0.5) (SD) μm	d(v,0.9) (SD) μm
large size (intact)	213.93 (8.50)	429.89 (10.97)	758.79 (18.13)
medium size (passed through sieve opening 75 – 150 μm)	83.80 (0.32)	150.80 (0.42)	259.39 (0.81)
small size (passed through sieve opening 38 – 75 μm)	4.24 (2.83)	63.88 (11.25)	123.13 (7.32)

2. Solid state characterization of hydrated beclomethasone dipropionate (prior to desolvation)

2.1 Appearance and morphology

Appearance and morphology of intact crystals (large size) and ground crystals (medium and small sizes) were characterized by scanning electron microscopy and light microscopy.

2.1.1 Particle size analysis

These three groups of crystals were measured for their particle sizes using laser particle size analyzer and the results are shown in Table 4 with the size distribution profiles in Appendix B (Figures 43-47). Size distribution curve of the particles of the smallest size shows that they were more polymodal dispersion and had high smaller size portion due to electrostatic effect of the particles, leading to a retention of small particles on the smallest sieve (38μm).

2.1.2 Scanning electron microscopy

Intact crystals (large size) are of columnar in habit. They are rod-like particles having a width and thickness exceeding that of needle-type particles. Figure 9A shows appearance of this kind of crystal. Figure 9B illustrates the crystals of medium size. They are columnar even though some shows irregular shape due to shearing effect after grinding. Irregular shape particles are observed more in the small size (Figure 9C), as a result of a longer grinding effect.

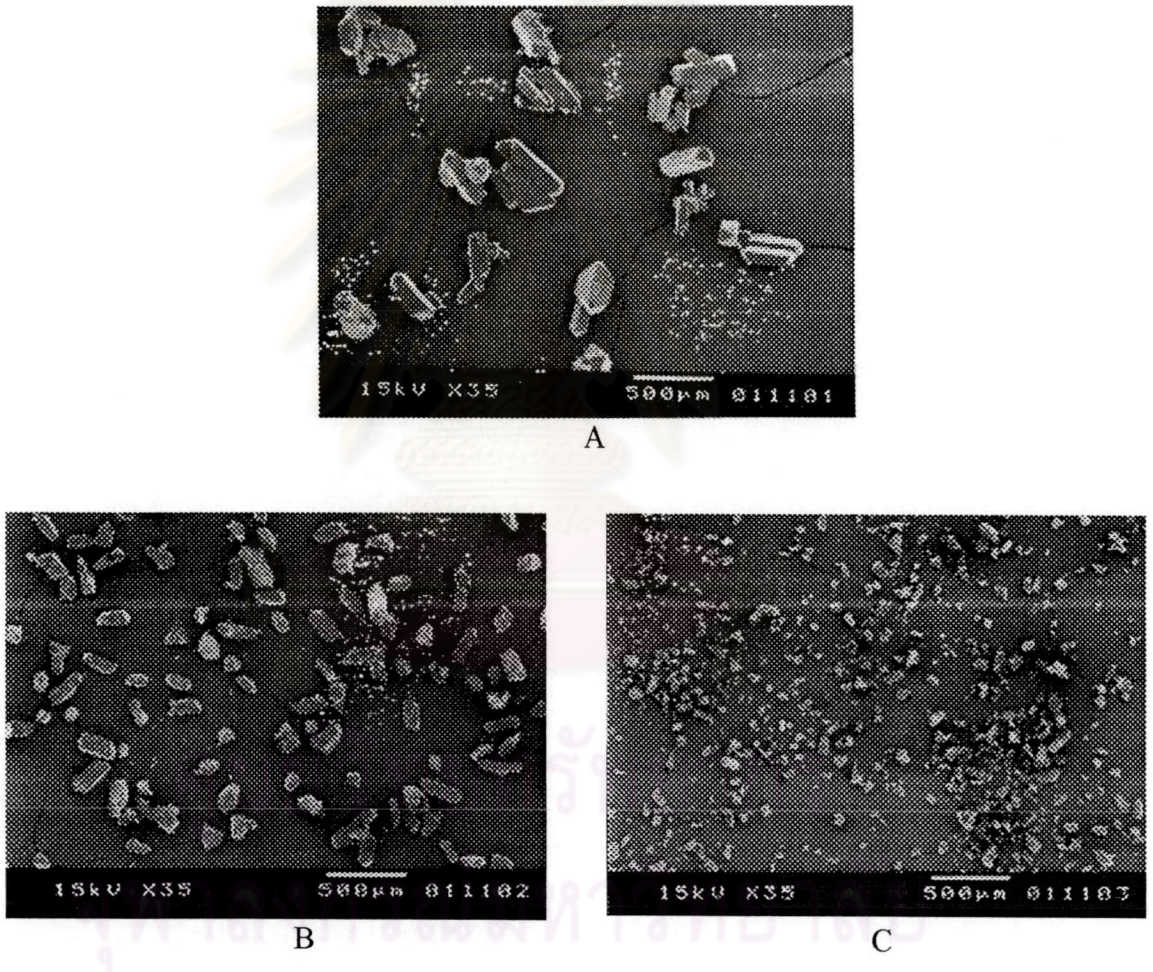

Figure 9 Scanning electronmicrographs of different sizes of hydrated beclomethasone diproprionate; A) large size (intact crystal); B) medium size (75-150µm crystal); C) small size (38-75µm crystal)

A

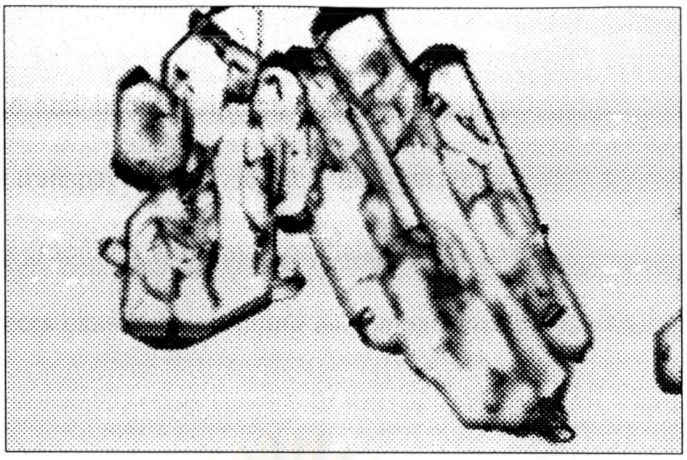

B

C

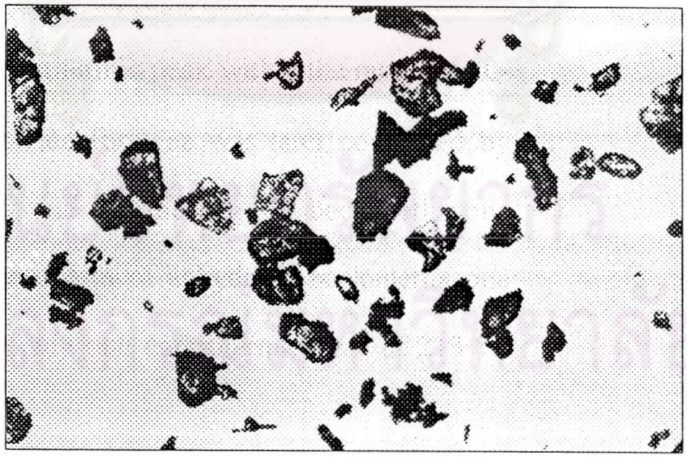

Figure 10 The photomicrographs of hydrated beclomethasone dipropionate observed by light microscope ×100; A) large size (intact crystal); B) medium size (75-150μm crystal); C) small size (38-75μm crystal)

2.1.3 Light microscopy

Figure 10 shows the appearance and habit of intact crystals by using ordinary light microscope, the crystals were transparent and looked like perfectly grown crystals. The surface of ground crystals (medium and small particles) prior to desolvation appeared dark implying crystal defects caused by grinding as compared to intact crystals (large particles).

2.2 Thermal and spectroscopic characterization of hydrated beclomethasone dipropionate

Solid state characteristics of the intact crystal (large size) and ground crystals (medium and small size) were obtained by differential scanning calorimetry (DSC), thermogravimetric analysis (TGA) and x-ray powder diffraction analysis (XRPD).

2.2.1 Thermal methods of analysis (DSC and TGA)

Differential scanning calorimetry (DSC) thermograms obtained from the three different sizes of hydrated beclomethasone dipropionate at a heating rate of 10 °C/min are shown in Figure 11. The first endothermic peak within the range of 80-120 °C indicated that the crystals were in solvate form as was later confirmed by TGA. The second endothermic peak was due to melting of beclomethasone dipropionate, corresponding to the melting endotherm of anhydrous beclomethasone dipropionate where there is a flat baseline and only one endothermic peak at 213 °C (Figure 12).

Further studies by thermogravimetric analysis (TGA) at a heating rate of 10 °C/min (see Appendix D in Figures 66 and 67) confirmed that there were weight loss from the crystals during the range of 80–120 °C, suggesting that solvent was

removed from the crystal lattice during that temperature range. Ensuring that the crystals obtained was stoichiometrically hydrated.

From the TGA thermograms in Appendix D, it was found that the intact and ground samples (prior to sieving) had an average weight loss of approximately 3.3% as shown in Table 5.

Table 5 Data of % weight loss of hydrated beclomethasone dipropionate obtained from TGA thermograms

Hydrated crystal	% weight loss			% average
	n_1	n_2	n_3	
Intact	3.5	3.2	3.3	3.3
Ground	3.4	3.4	3.2	3.3

To calculate the ratio of water to drug, the mass of each component must first be calculated and the number of moles of water to drug was determined following this equation:

$$\frac{\text{mole water}}{\text{mole drug}} = \frac{\text{(grams water lost)/(18 g/mole)}}{\text{(grams sample-grams water lost)/(molecular weight of drug)}}$$

$$\frac{\text{mole water}}{\text{mole drug}} = \frac{(3.3)/(18\ \text{g/mole})}{(100-3.3)/(521.1)} = 1$$

The percent weight change of the monohydrate, corresponded to the theoretical change of 3.34% in weight, and was calculated from,

Molecular weight of water/beclomethasone dipropionate monohydrate = 18/539.1*100

= 3.34%

Note: Molecular weight of beclomethasone dipropionate : 521.1

Molecular weight of beclomethasone dipropionate monohydrate : 539.1

Molecular weight of water : 18

The results from this study show that the percent weight loss of solvent of the compounds is approximately equal to the theoretical weight change of beclomethasone dipropionate monohydrate which is 3.34%, and amount of weight loss of solvent is a mole of water per mole of drug, indicating that the compound was beclomethasone dipropionate in monohydrate form.

The result from the DSC thermograms of each sample previously shown in Figure11, indicated that the temperature for the endothermic of dehydration peak at 80-120 °C were higher with decreasing particle size. Investigation of ground samples, before being suspended in the water, employing DSC instrument revealed a higher dehydration temperature than that of intact crystal. This higher dehydration temperature was the result of crystal imperfection due to the grinding process. The DSC curves (Figure 13) show the same dehydration temperatures after grinding, both before and after suspension process. As a result, it is possible that the resuspension can only convert partial amorphous phase, which may occur during grinding process, to ensure crystallinity of the sample. But the structure of dehydrated form (anhydrous) resulting from crystal imperfection at the surface cannot be converted to hydrated form by resuspension process. This result is similar to that of Nacheingtung (1997) that the rehydration did not occur when the structure of hydrated beclomethasone dipropionate was dehydrated and collapsed to anhydrous form.

One reason for the increase in dehydration temperature is that the grinding process may produce thin layer of dehydrated portion on the surface of the samples. Dehydration may occur at the surface of the crystal producing a shield of

protection against further water loss from the inside of particles which for the purpose of this thesis will call "surface barrier effect". This shield or barrier then hindered water removal from the crystal resulting in a higher dehydration endothermic temperature. This surface barrier effect was confirmed when a non-transparent portion of ground crystals was observed under a light microscope (Figure 10). The same result has been shown in dehydration of hydrated caffeine, which resulted in non-transparent (opaque) crystals (Byrn, 1999).

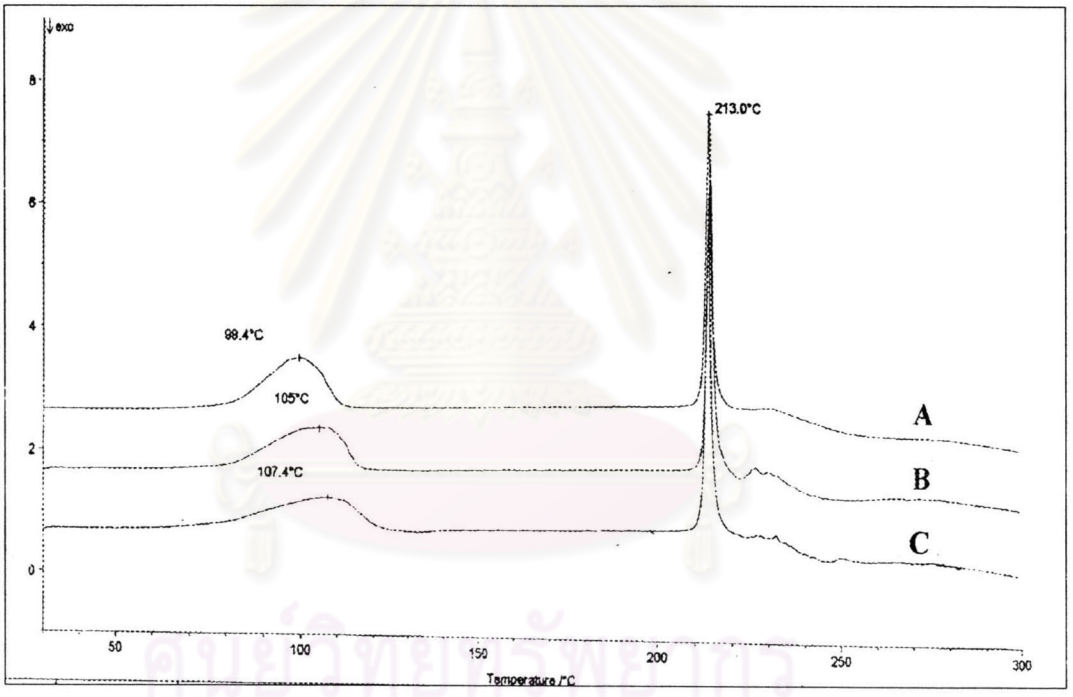

Figure 11 The DSC curve of hydrated beclomethasone dipropionate at scanning rate 10°C/min; A: large crystals (intact); B: medium crystals (75-150 μm); C: small crystals (38-75 μm)

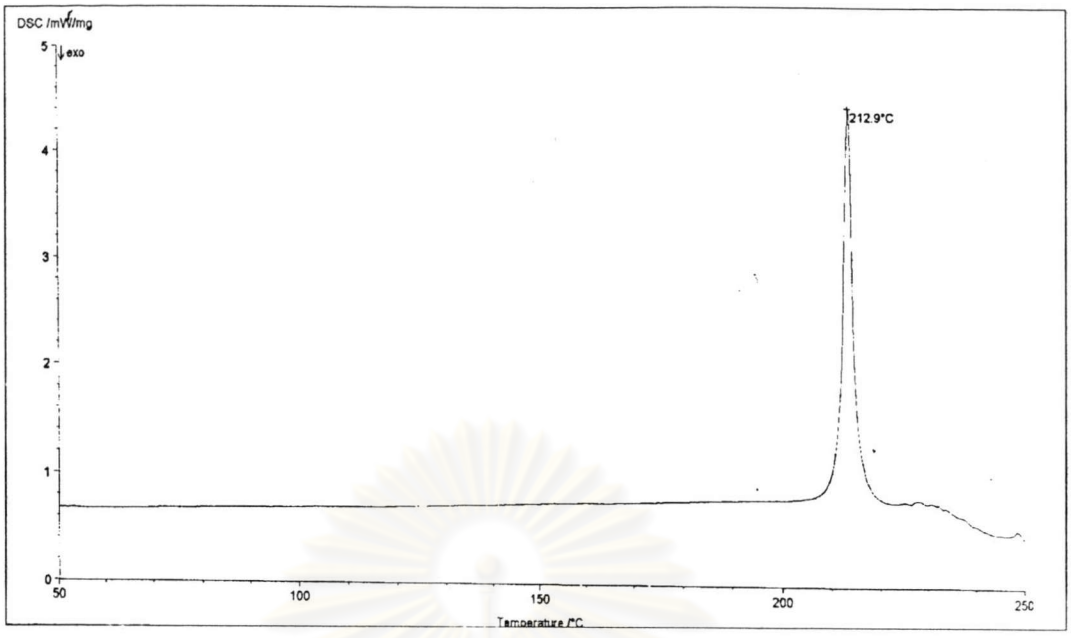

Figure 12 The DSC curve of anhydrous beclomethasone dipropionate at scanning rate of 10°C/min

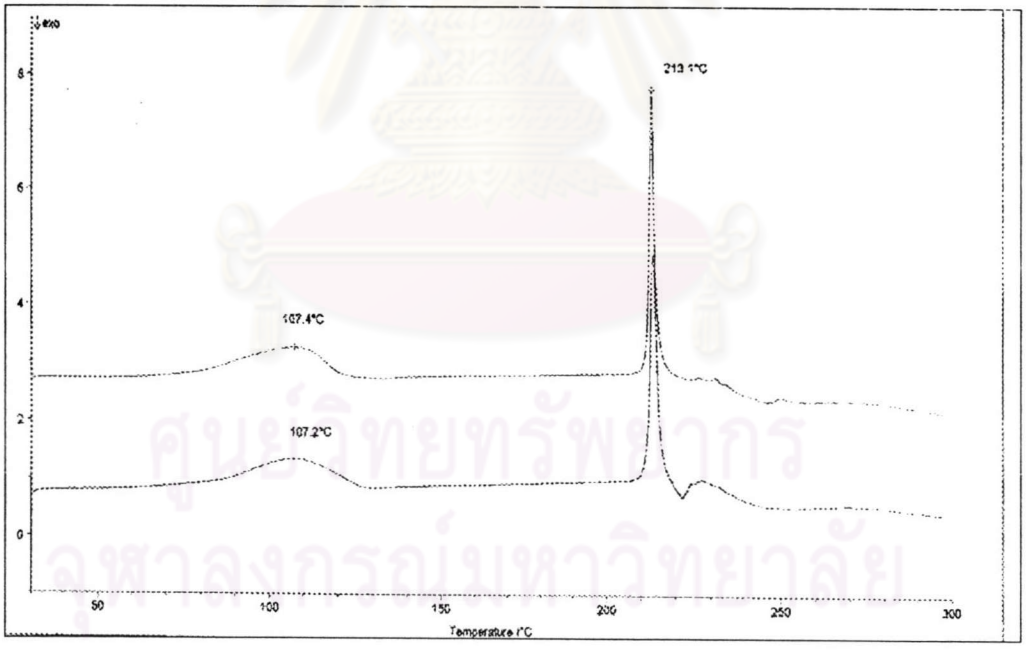

Figure 13 The DSC curve at scanning rate of 10°C/min of hydrated form
Top: after suspending; Bottom: before suspending (after grinding)

The diagram of "surface barrier effect" occurred by grinding may be explained as follow.

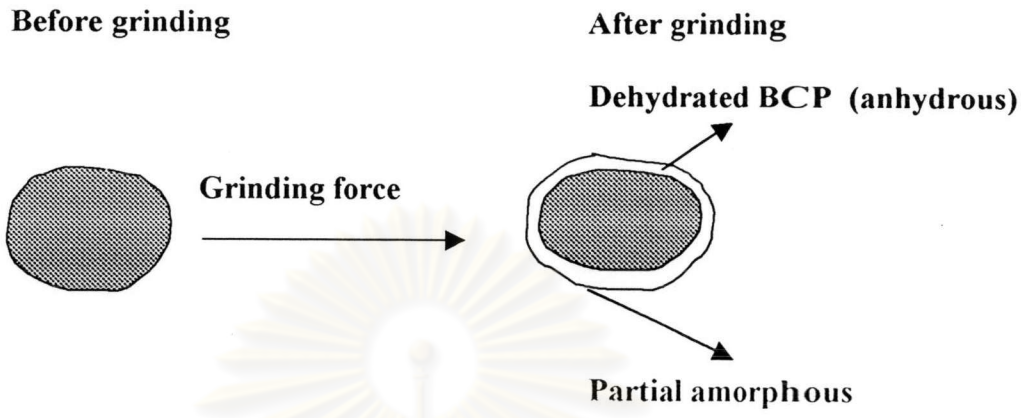

2.2.2 Qualitative x–ray powder diffraction analysis

X-ray powder diffraction patterns of all three samples of different sizes of beclomethasone dipropionate monohydrate form correlate well with standard powder diffraction file (PDF Standard from Nachiengtung, 1997) (Figure 14). The low peak intensities of the small size might be due to the effect of grinding since it decreased the crystallinity of the crystal either by turning it into a partially amorphous solid and/or the effect of size on the intensities of the diffracted x-ray beam itself (the smaller particles show broader and lower diffracted x-ray intensities) (Kitamura et al, 1989). Since in the previous experiment resuspension to ensure conversion to crystallinity, hence, the former reason was not the prominent cause in this case. Thus, size played a major role in the peak intensity reduction observed.

The monohydrate form has high intensity peaks at °2θ = 8.380°, 12.355°, 14.455°, 16.480° and 17.445° while the anhydrous form of beclomethasone dipropionate has strong peaks at °2θ = 9.685°, 11.420°, 14.685°, 15.660° and 18.485° (Figure 15). The distinctively different peak positions in the x–ray powder diffraction patterns indicate that water of hydration plays a major role in crystal lattice arrangements and packing of beclomethasone dipropionate molecules. For identification of phase interconversion between these two forms, peak positions at 8.380° of hydrated form and 18.485° of anhydrous form were selected for the future studies. (see Section 3.2).

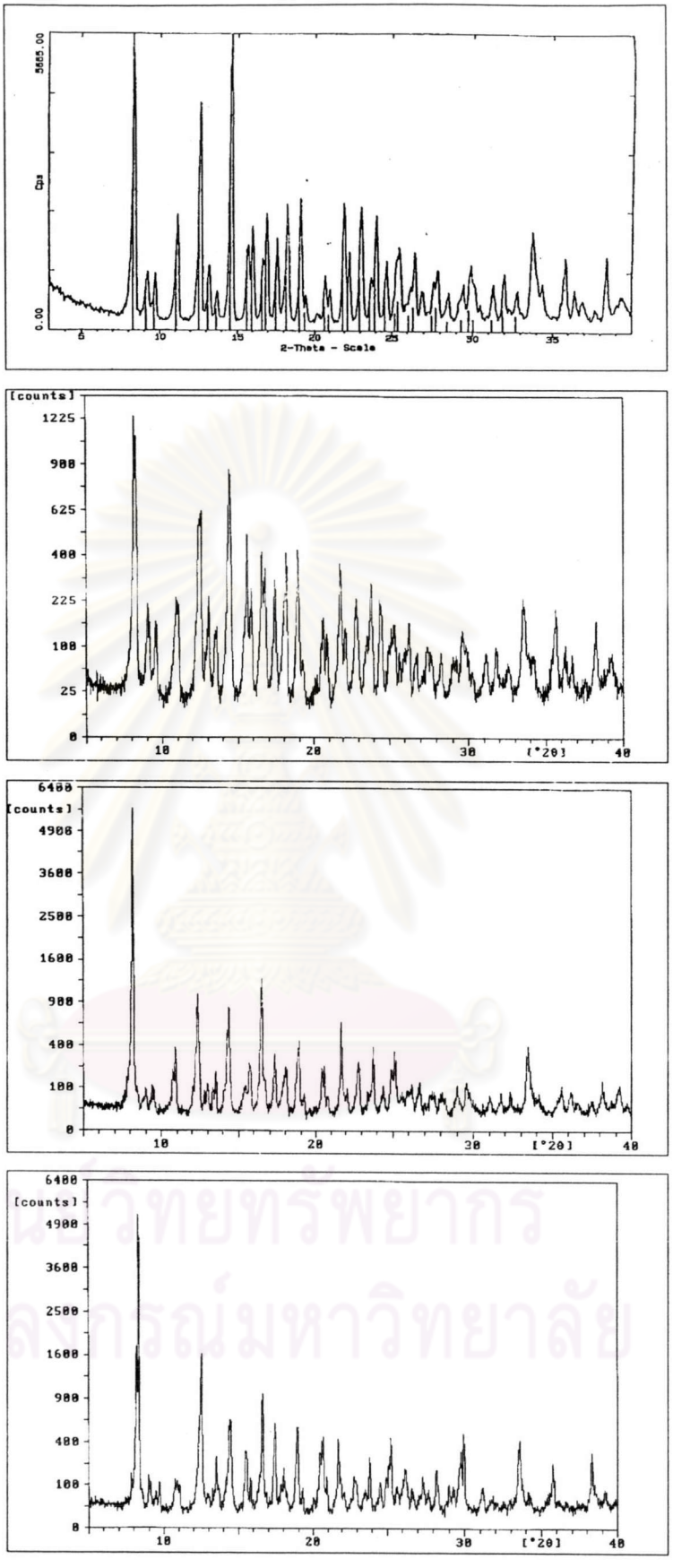

Figure 14 The x-ray spectra of beclomethasone dipropionate monohydrate
A: PDF standard; B small crystals; C. medium crystals, D: large crystals

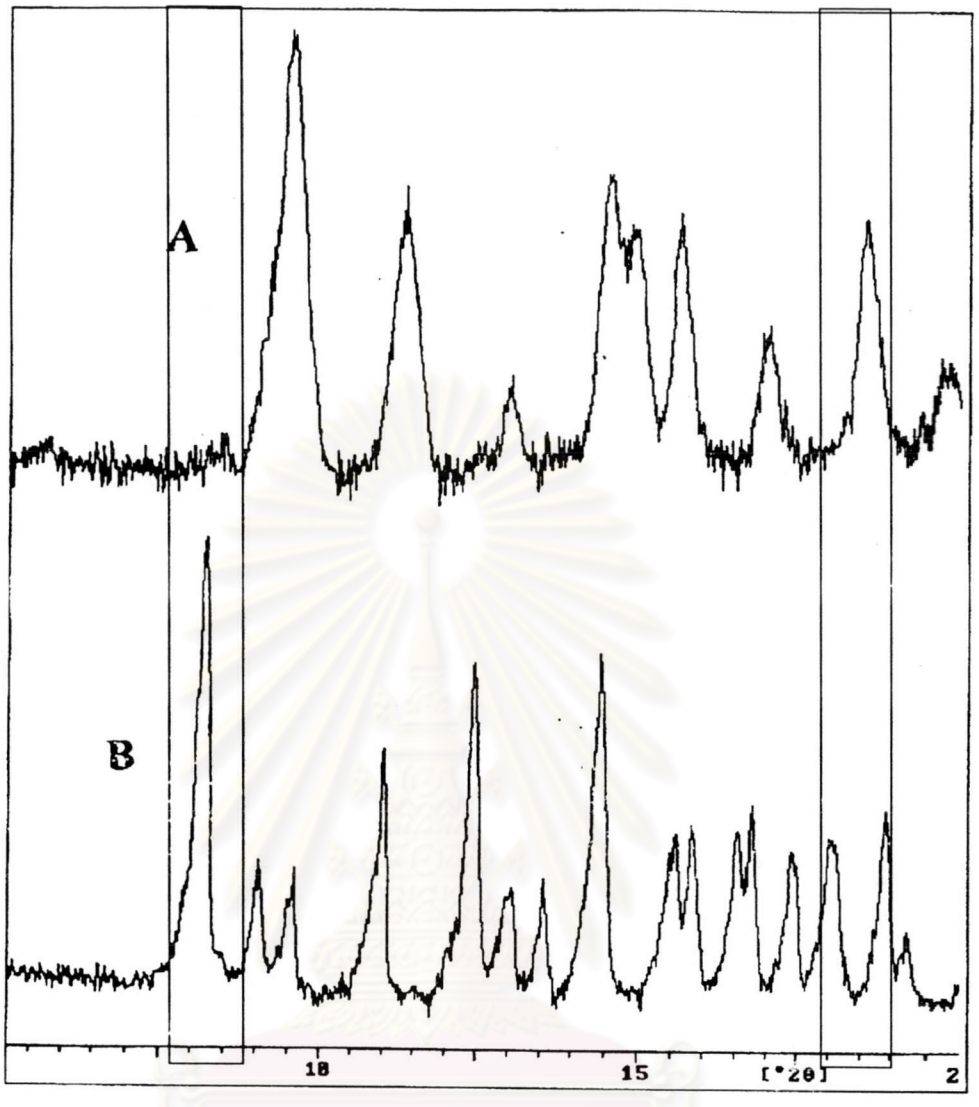

Figure 15 Comparison of x-ray spectra of beclomethasone dipropionate

A) anhydrous form

B) monohydrate form

Figure 16 shows the x-ray powder diffraction patterns of ground samples (medium and small sizes) before being suspended in water (Figure 16A) as compared to intact crystals (large size) (Figure 16B). Their patterns appeared to be the same at every °2θ positions. Two reasons are possible, either the anhydrous that was assumed to form on the surface of ground crystals was so minute (approximately less than 10%w/w) and was below the limit of detection of x-ray powder diffractometer to differentiate the ground samples from the intact one or the removal of water on the surface of crystals resulted in waterless cavities but was insufficient to cause further structural rearrangement to the anhydrous form.

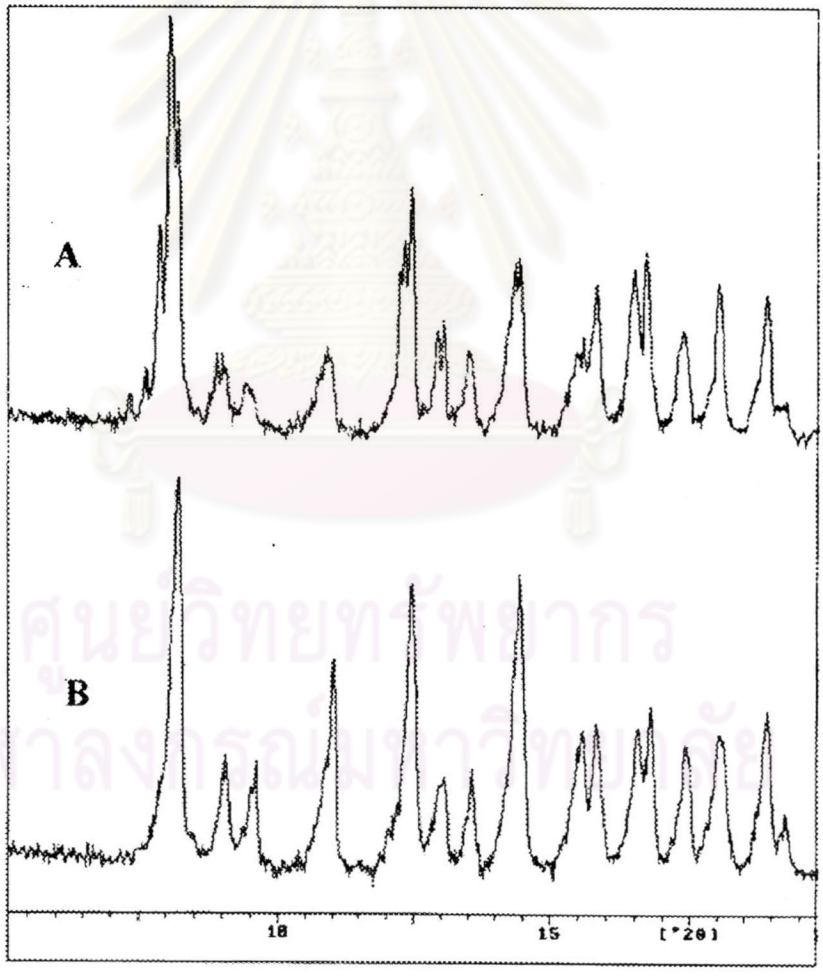

Figure 16 X-ray spectra of ground and intact crystals
A: ground crystal; B: intact crystal

3. Dehydration process for particle size reduction of hydrated beclomethasone dipropionate

3.1 Solvent stability

The plots of percent fraction of isothermal dehydration (as calculated by the ratio between percent weight loss of sample and theoretical percent amount of water in the stoichiometric hydrated crystal) versus the times required for dehydration of all three samples are shown in Figures17, 18, and 19. From these three figures, it was found that for the large particles, induction period for water removal, which is the equilibrium of outside temperature and the temperature of the particle, was longer. This was probably due to the increasing surface area of the smaller particle size that promotes initial rapid water removal (Agbada and York, 1994). The temperatures used were increased in order to overcome the dehydrated barrier in the ground samples (medium and small particles) than the large particle due to initial imperfection of the surface during grinding as mentioned in the previous section while this effect was lacking in the large particle. The surface was assumed to be anhydrous while the interior of the particle remained as monohydrated form. Therefore, "the surface barrier" on the surface of ground crystals acted as a shield and prevented water removal from inside of particle as discussed previously. Moreover, the higher vapor pressure in the large size promoted the diffusion of water as could be visualized in Figure 20.

Also from Figures 17, 18, and 19, the rates of desolvation increased with the increment of temperatures. However, the higher temperature applied to each samples (85.5°C for the large and medium particles) did not lead to the higher rate of dehydration. It could be explained that the higher temperature generated the dehydrated barrier on the surface of particle as more compacted anhydrous form of beclomethasone dipropionate. While at the beginning of dehydration, the lower

temperatures could not rearrange the monohydrate form to the more compacted anhydrous form. This shield blocked water removal, and the dehydration of samples could not proceed higher than normal at the temperature stated above. This effect was intensified with the medium size particles due to already existing anhydrous barrier after grinding. Besides, in the large particles, more water was retained. Vapor pressure generated in particles could diffuse through the compact anhydrous barrier and overcome the surface barrier effect. On the other hand, the medium particles had less water retained in the lattice, the crystal had slower dehydration rate at higher temperature (85.5 °C) compared to intact crystals. The water from the medium crystals could not be removed from the crystal nuclei as indicated by the lower equilibrium %fraction dehydration, which was only 80% in 90 min (Figure 18). It was assumed that, at a greater temperature (in this case, 85.5 °C), the surface of the particles may loose water faster than the inside and collected more thermal energy causing the dehydrated structure to collapse and blocked the channels for water removal. In addition to a shield resulting from dehydration at high temperature, medium particles already possessed a shield produced by grinding process. Therefore, it seemed like medium particles had additional layers of barrier on the surface. Besides, the water retained inside the medium particle was so minute that it could not generate vapor pressure high enough to overcome the dehydrated barrier. Hence, the data for 85.5 °C of the medium particle was not used for the kinetic parameter determination.

There seemed to be two mechanisms for dehydration of the small size particles. These two mechanisms worked at two different ranges of temperatures, i.e. at 80 and 85.5 °C, and higher than 85.5 °C (101.5 °C and 90.5 °C). At the temperature 85.5 °C and lower, growth rate of the anhydrous barrier impeding inward occurred at almost the same rate as water diffusion. At higher temperatures used (101.5 °C and 90.5 °C) promoted movement of the water molecules as shown by a higher rate of dehydration which was assumed to be a result of the generation of

metastable higher energetic state (amorphous form) on the surface of the particle. These temperatures should not be used in size reduction due to the induction of a phase change to higher energetic state resulting in a significant decrease in physical and chemical stability (Ito et al., 1996; Kitamura et al., 1989).

With the four temperatures employed (80, 85.5, 90.5, 101.5 °C), dehydration of small particle seemed to be separated into two groups of mechanism. Due to the fact that this event was unexpected and only two data points are not sufficient for further analysis. The temperature of dehydration of 74.5 °C was then applied to small particle using TGA to confirm the mechanism and to identify the possible activation energy at low temperature.

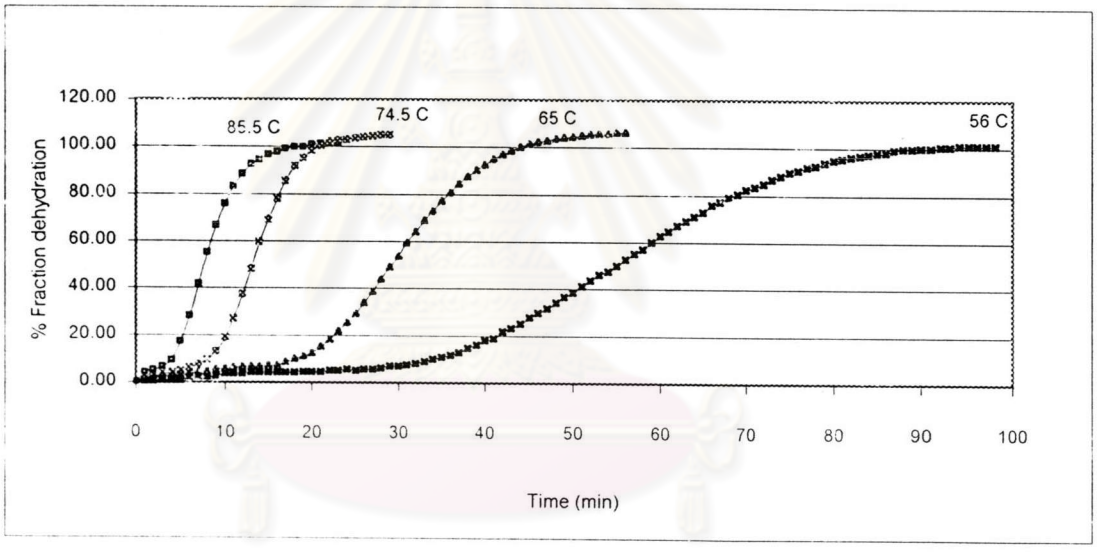

Figure 17 The isothermal dehydration of intact beclomethasone dipropionate monohydrate (large particles)

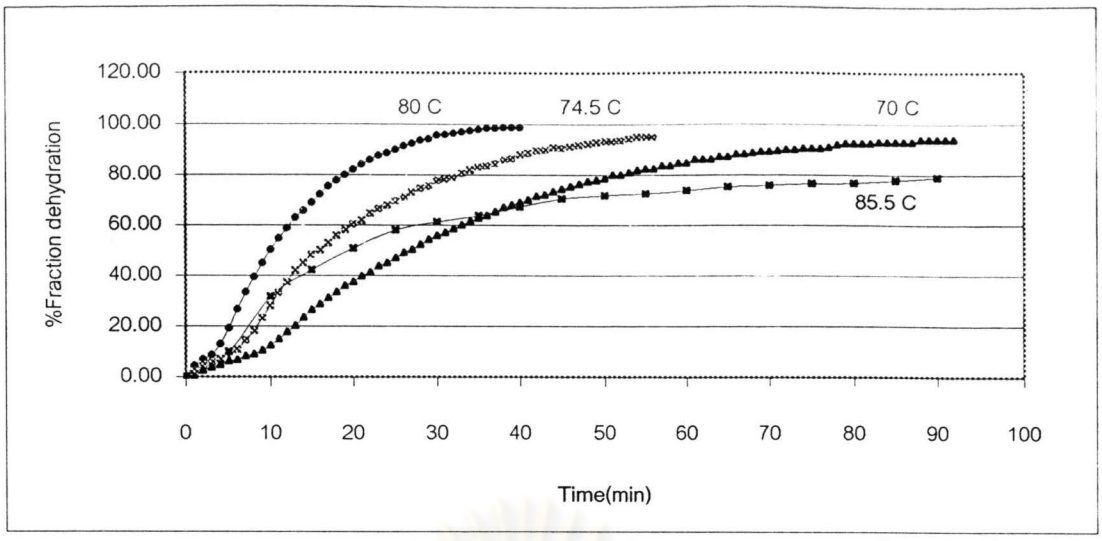

Figure 18 The isothermal dehydration of medium crystals of beclomethasone dipropionate monohydrate

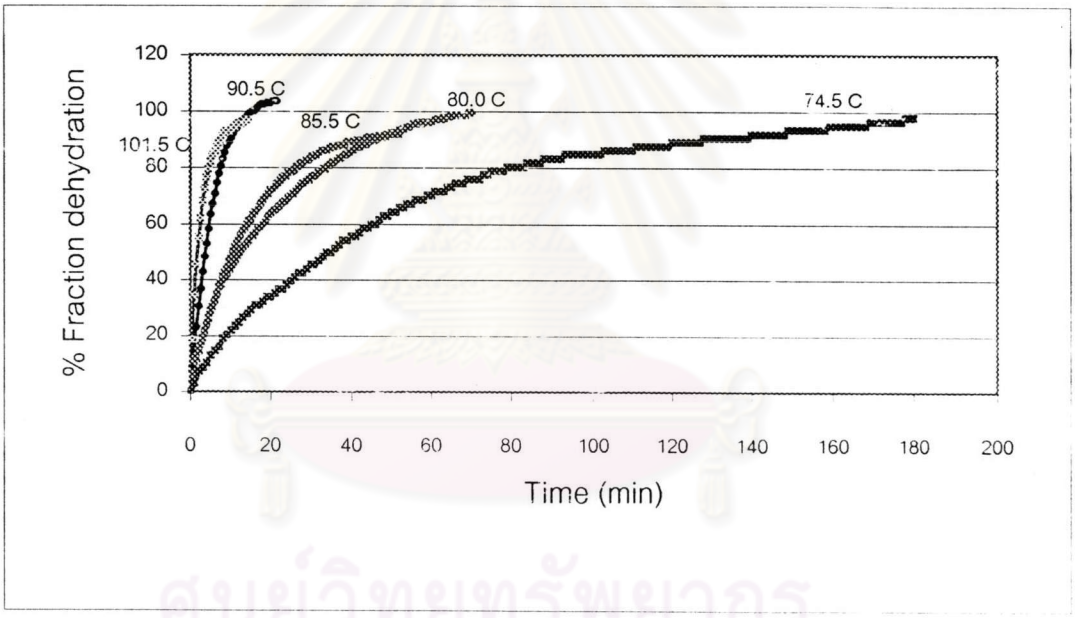

Figure 19 The isothermal dehydration of small crystals of beclomethasone dipropionate monohydrate

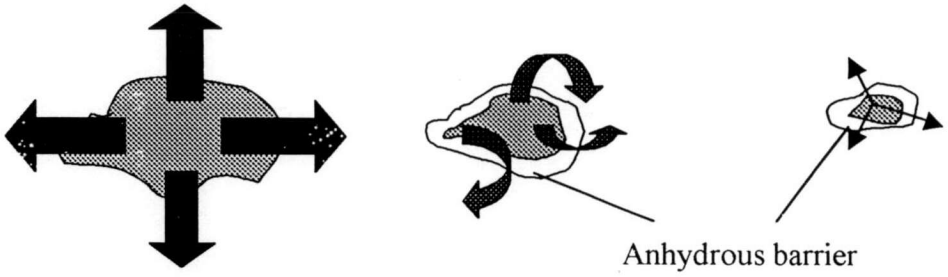

A
Large particle

B
Medium particle

C
Small particle

Figure 20 Effect of anhydrous barrier on dehydration
(Arrows refer to vapor pressure driving force inside the particle.)

To determine which kinetic equations were best fitted, the correlation of determination (R^2) was calculated. Employing kinetic equations shown in Table 2, rate constants and the correlation of coefficient obtained from each reaction are calculated and demonstrated in Table 6 for the large particles (intact crystals), Table 7 for the medium particles, and Table 8 for the small particles.

Correlation of determination (R^2) described in Tables 6, 7, and 8 show that the dehydration data for all samples seem to fit with the Avrami-Erofeev equation. However, Byrn (1999) stated, "The fact that more than one equation fits the data indicated that solid-state kinetic data cannot be used to prove the mechanism of solid-stated reaction. Nevertheless it is important for the determination of the activation energy to select the proper kinetic equation.". Thus, the Arrhenius plots for all samples were chosen from the best fitted equation with the highest correlation of determination (R^2). The best fitted dehydration data for ground samples, the medium and small particles, followed the Avrami-Erofeev equation (n=1), while the intact particles expressed the model of Avrami-Erofeev equation (n=1/3). For the Avrami-Erofeev model, it is assumed that volumes within the solid at a given time are activated, and n being the proportion of the numbers of nuclei. The model is shown in Figure 8 previously.

Table 6 Data and mechanisms for isothermal dehydration of "large particles" beclomethasone dipropionate monohydrate obtained at various temperatures (intact crystals)

Mechanisms	85.5 ℃		74.5 ℃		65.0 ℃		56.0 ℃	
	$k(min^{-1})$	R^2	$k(min^{-1})$	R^2	$k(min^{-1})$	R^2	$k(min^{-1})$	R^2
Reactions involving nucleation								
• Linearly growing nuclei Prout-Tompkins	*0.5252*	*0.9952*	*0.4525*	*0.9997*	*0.2088*	*0.9999*	*0.0992*	*0.9994*
• Random nuclei								
Avrami-Erofeev, n = 1/4	*0.0830*	*0.9925*	*0.0725*	*0.9992*	*0.0334*	*0.9996*	*0.0159*	*0.9995*
n = 1/3	***0.1072***	***0.9962***	***0.0930***	***0.9998***	***0.0432***	***0.9997***	***0.0206***	***0.9996***
n = 1/2	*0.1518*	*0.9997*	*0.1297*	*0.9979*	*0.0614*	*0.9972*	*0.0292*	*0.9972*
n = 2/3	*0.1927*	*0.9980*	*0.1619*	*0.9922*	*0.0779*	*0.9914*	*0.0371*	*0.9916*
n = 1	*0.2684*	*0.9817*	*0.2169*	*0.9706*	*0.1075*	*0.9710*	*0.0512*	*0.9715*
Reaction controlled by phase boundaries								
• One-dimensional phase boundary(zero-order mechanism)	*-0.1137*	*0.9919*	*-0.1014*	*0.9982*	*-0.0474*	*0.9982*	*-0.0226*	*0.9990*
• Two-dimensional phase boundary	*0.0856*	*0.9979*	*0.0731*	*0.9921*	*0.0352*	*0.9927*	*0.0168*	*0.9932*
• Three-dimensional phase boundary	*0.0660*	*0.9951*	*0.0554*	*0.9867*	*0.0269*	*0.9873*	*0.0129*	*0.9878*
Diffusion controlled reaction								
• One-dimensional diffusion	*0.1160*	*0.9860*	*0.0980*	*0.9714*	*0.0485*	*0.9774*	*0.0233*	*0.9785*
• Two-dimensional diffusion	*0.0888*	*0.9669*	*0.0717*	*0.9470*	*0.0363*	*0.9545*	*0.0173*	*0.9554*
• Three-dimensional diffusion (Ginstling-Brounshtein)	*0.0234*	*0.9554*	*0.0185*	*0.9348*	*0.0094*	*0.9425*	*0.0045*	*0.9433*
• Three-dimensional diffusion (Jander equation)	*0.0328*	*0.9282*	*0.0248*	*0.9080*	*0.0129*	*0.9155*	*0.0061*	*0.9165*
Other equations								
• First order	*0.2568*	*0.9256*	*0.2357*	*0.9651*	*0.1013*	*0.9701*	*0.0480*	*0.9698*
• Second order	*0.7490*	*0.8850*	*0.5192*	*0.8851*	*0.2737*	*0.8809*	*0.1288*	*0.8833*

Table 7 Data and mechanisms for isothermal dehydration of" medium particles" of beclomethasone dipropionate monohydrate obtained at various temperatures (ground crystal)

Mechanisms	*80.0 ℃*		*74.5 ℃*		*70.0 ℃*	
	k(min⁻¹)	*R^2*	*k(min⁻¹)*	*R^2*	*k(min⁻¹)*	*R^2*
Reactions involving nucleation						
• Linearly growing nuclei Prout-Tompkins	*0.1873*	*0.9727*	*0.1005*	*0.9668*	*0.0661*	*0.9799*
• Random nuclei						
Avrami-Erofeev, n = 1/4	*0.0298*	*0.9678*	*0.0160*	*0.9600*	*0.0106*	*0.9754*
n = 1/3	*0.0387*	*0.9755*	*0.0209*	*0.9676*	*0.0138*	*0.9816*
n = 1/2	*0.0553*	*0.9876*	*0.0303*	*0.9801*	*0.0197*	*0.9910*
n = 2/3	*0.0707*	*0.9954*	*0.0392*	*0.9894*	*0.0253*	*0.9969*
n = 1	***0.0988***	***0.9992***	***0.0559***	***0.9985***	***0.0355***	***0.9990***
Reaction controlled by phase boundaries						
• One-dimensional phase boundary (zero-order mechanism)	*-0.0422*	*0.9715*	*-0.0230*	*0.9593*	*-0.0151*	*0.9770*
• Two-dimensional phase boundary	*0.0319*	*0.9941*	*0.0177*	*0.9865*	*0.0114*	*0.9957*
• Three-dimensional phase boundary	*0.0245*	*0.9979*	*0.0137*	*0.9923*	*0.0088*	*0.9986*
Diffusion controlled reaction						
• One-dimensional diffusion	*0.0444*	*0.9990*	*0.0253*	*0.9955*	*0.0161*	*0.9990*
• Two-dimensional diffusion	*0.0336*	*0.9954*	*0.0194*	*0.9991*	*0.0122*	*0.9953*
• Three-dimensional diffusion (Ginstling-Brounshtein)	*0.0088*	*0.9909*	*0.0051*	*0.9979*	*0.0032*	*0.9910*
• Three-dimensional diffusion (Jander equation)	*0.0121*	*0.9772*	*0.0070*	*0.9910*	*0.0044*	*0.9786*
Other equations						
• First order	*0.0885*	*0.8786*	*0.0446*	*0.8733*	*0.0306*	*0.8999*
• Second order	*0.2579*	*0.9547*	*0.1492*	*0.9753*	*0.0919*	*0.9584*

Table 8 Data and mechanisms from isothermal dehydration of "small particle"beclomethasone dipropionate monohydrate obtained at various temperatures (ground crystal)

Mechanisms	***101..5 ℃***		***90.5 ℃***		***85.5 ℃***		***80.0 ℃***		***74.5℃***	
	k(min^{-1})	***R^2***	***k(min^{-1})***	***R^2***	***k(min^{-1})***	***R^2***	***k(min^{-1})***	***R^2***	***k(min^{-1})***	***R^2***
Reactions involving nucleation										
• Linearly growing nuclei Prout-Tompkins	*0.6112*	*0.9377*	*0.4214*	*0.9896*	*0.0767*	*0.9719*	*0.0767*	*0.9719*	*0.0371*	*0.9829*
• Random nuclei										
Avrami-Erofeev, n = 1/4	*0.0962*	*0.9273*	*0.0670*	*0.9857*	*0.0173*	*0.9583*	*0.0122*	*0.9655*	*0.0059*	*0.9783*
n = 1/3	*0.1255*	*0.9399*	*0.0875*	*0.9903*	*0.0226*	*0.9660*	*0.0160*	*0.9724*	*0.0077*	*0.9836*
n = 1/2	*0.1813*	*0.9613*	*0.1261*	*0.9967*	*0.0327*	*0.9788*	*0.0233*	*0.9837*	*0.0111*	*0.9917*
n = 2/3	*0.2343*	*0.9777*	*0.1623*	*0.9995*	*0.0422*	*0.9884*	*0.0302*	*0.9917*	*0.0142*	*0.9966*
n = 1	***0.3368***	***0.9964***	***0.2303***	***0.9955***	***0.0602***	***0.9985***	***0.0434***	***0.9987***	***0.0200***	***0.9978***
Reaction controlled by phase boundaries										
• One-dimensional phase boundary(zero-order)	*-0.1334*	*0.9275*	*- 0.0954*	*0.9851*	*-0.0247*	*0.9564*	*- 0.0100*	*1.0000*	*-0.0085*	*0.9776*
• Two-dimensional phase boundary	*0.1041*	*0.9720*	*0.0731*	*0.9990*	*0.0191*	*0.9848*	*0.0136*	*0.9892*	*0.0064*	*0.9947*
• Three-dimensional phase boundary	*0.0812*	*0.9826*	*0.0565*	*0.9998*	*0.0148*	*0.9911*	*0.0106*	*0.9942*	*0.0500*	*0.9974*
Diffusion controlled reaction										
• One-dimensional diffusion	*0.1458*	*0.9864*	*0.1032*	*0.9984*	*0.0271*	*0.9931*	*0.0196*	*0.9969*	*0.0091*	*0.9963*
• Two-dimensional diffusion	*0.1142*	*0.9979*	*0.0790*	*0.9899*	*0.0208*	*0.9983*	*0.0151*	*0.9991*	*0.0069*	*0.9932*
• Three-dimensional diffusion	*0.0303*	*0.9990*	*0.0207*	*0.9834*	*0.0054*	*0.9978*	*0.0040*	*0.9971*	*0.0018*	*0.9895*
• Three-dimensional diffusion (Jander equation)	*0.0431*	*0.9949*	*0.0288*	*0.9662*	*0.0076*	*0.9922*	*0.0055*	*0.9887*	*0.0025*	*0.9782*
Other equations										
• First order	*0.2744*	*0.7981*	*0.1911*	*0.9190*	*0.0487*	*0.8715*	*0.0333*	*0.8820*	*0.0171*	*0.9111*
• Second order	*0.9776*	*0.9767*	*0.6210*	*0.9365*	*0.1618*	*0.9786*	*0.1176*	*0.9689*	*0.0521*	*0.9600*

Figures 21, 22 and 23 are the Avrami-Erofeev plots of the three sample sizes together with their respective Arrhenius plots (rate constant versus 1/T).

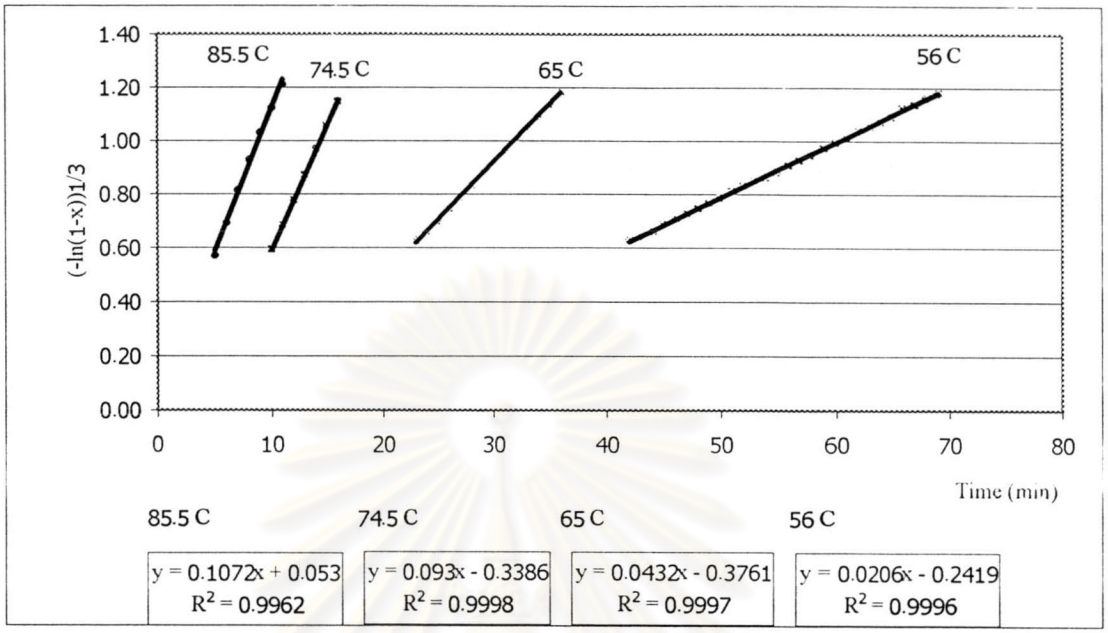

A

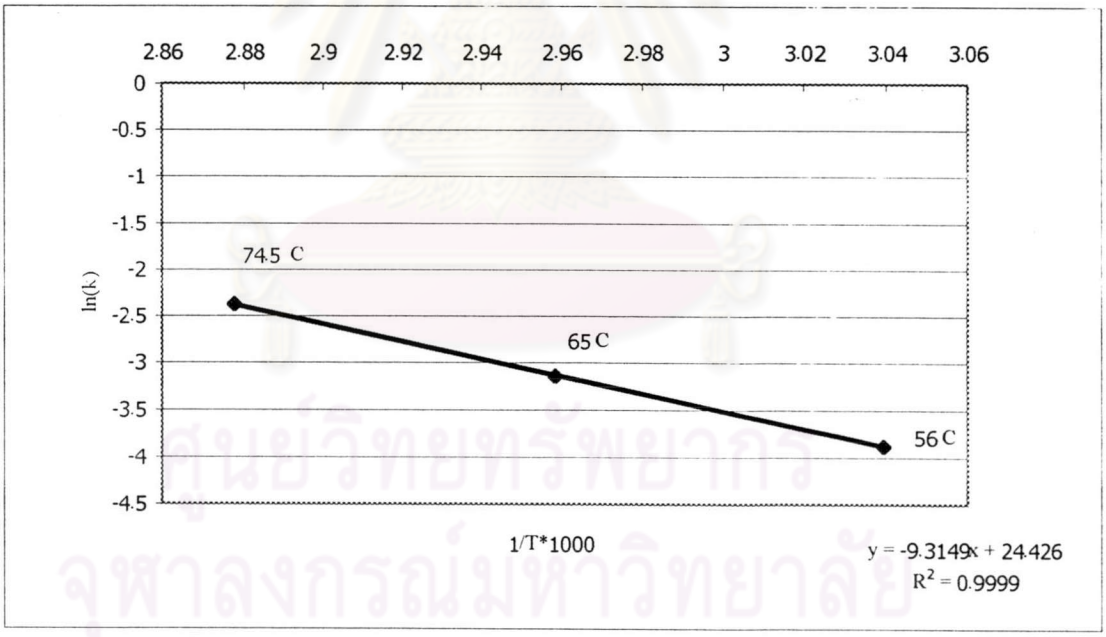

B

Figure 21 The Avrami-Erofeev and Arrhenius plots of large crystals

A: Avrami-Erofeev plot (n = 1/3)

B: Arrhenius plot

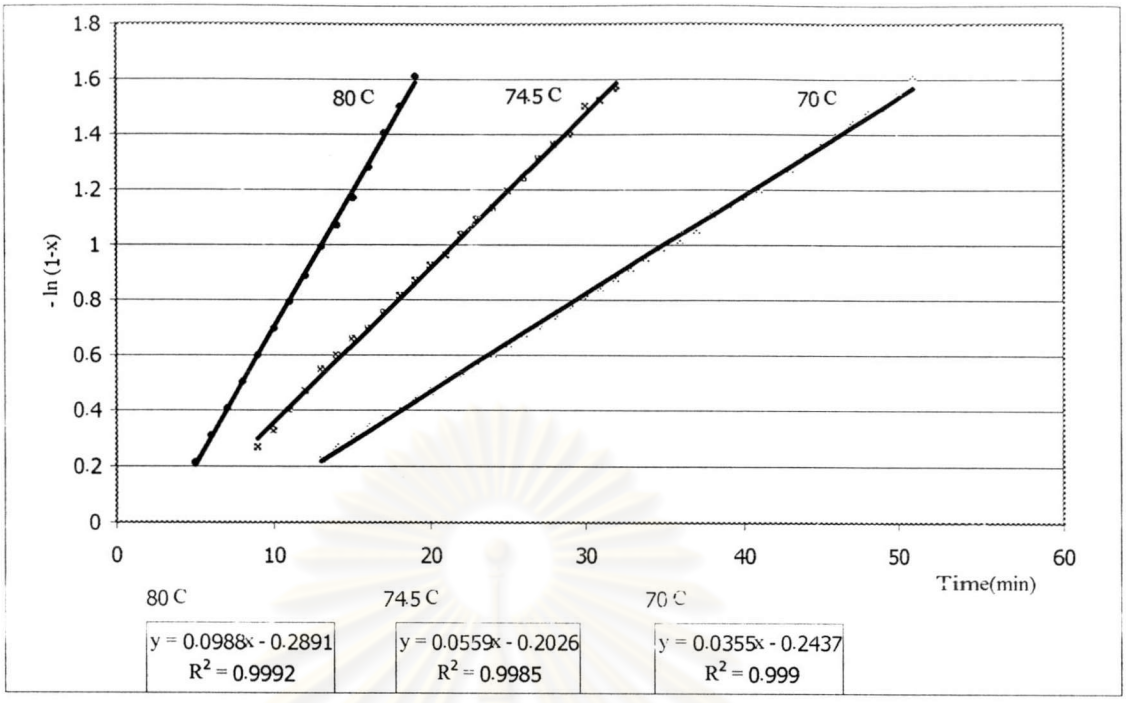

A

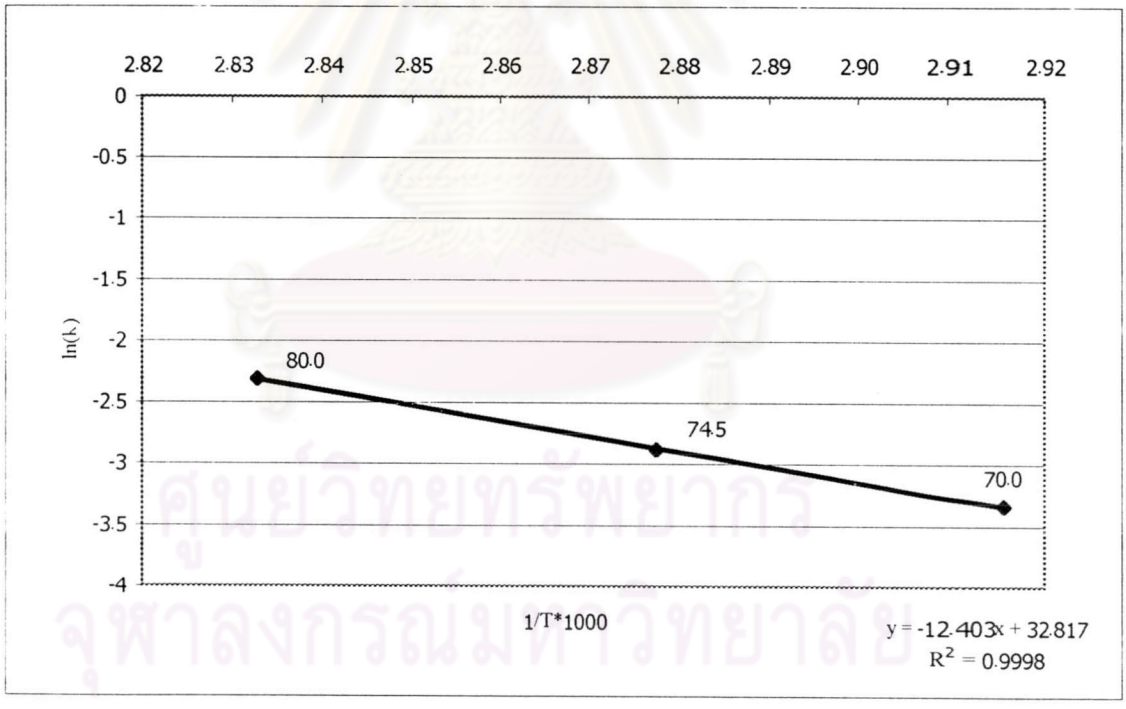

B

Figure 22 The Avrami-Erofeev and Arrhenius plots of medium crystals

A: Avrami-Erofeev plot (n = 1)

B: Arrhenius plot

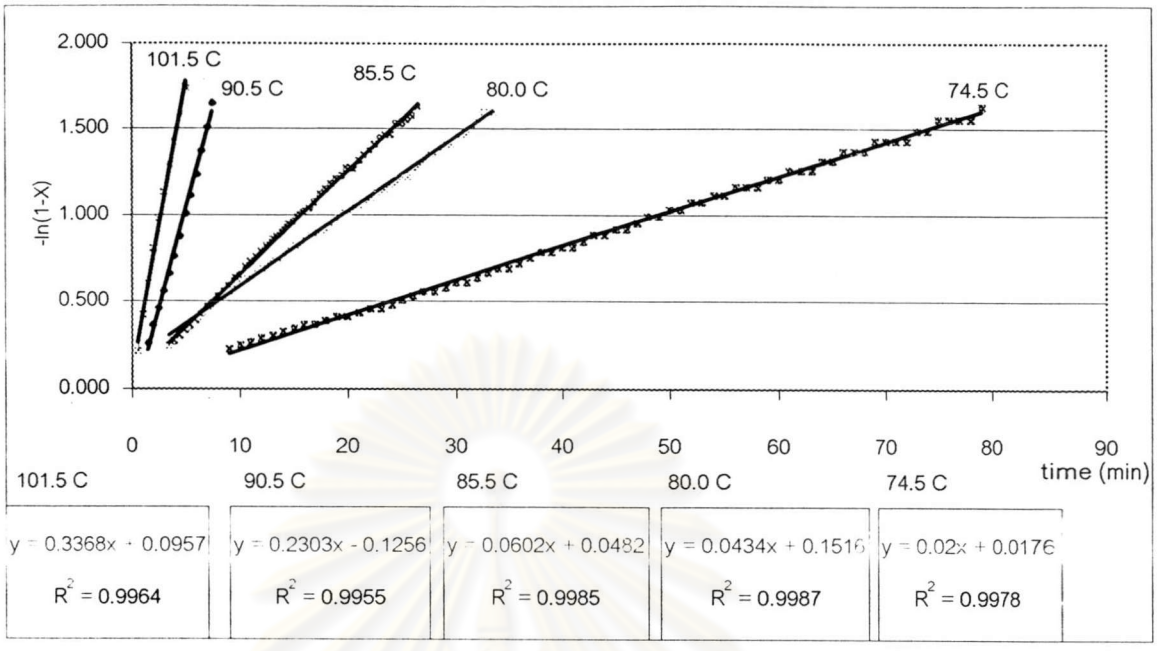

A

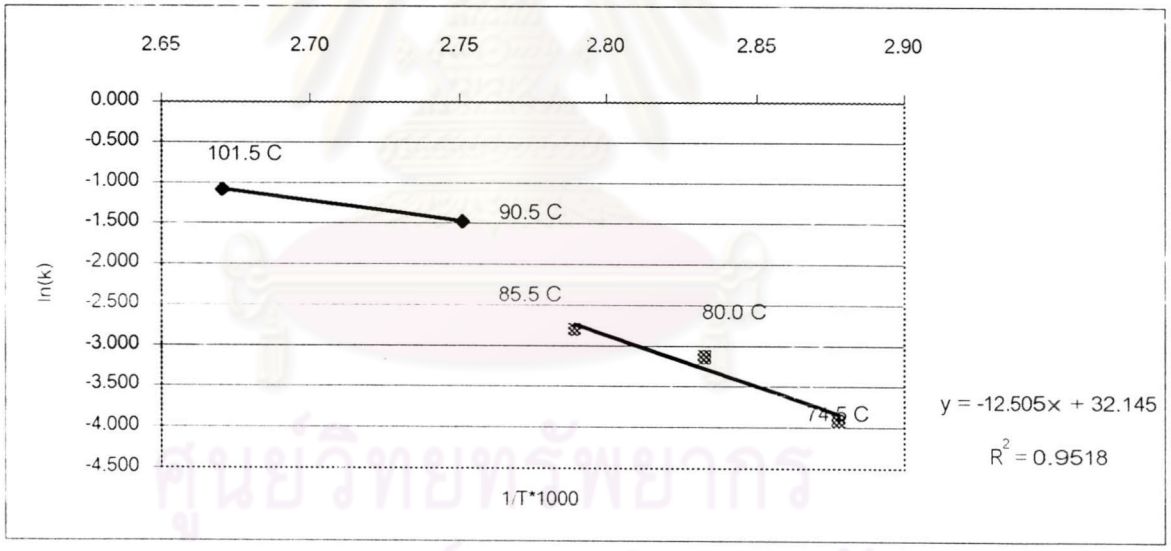

B

Figure 23 The Avrami-Erofeev and Arrhenius plots of small crystals

A: Avrami-Erofeev plot (n = 1)

B: Arrhenius plot

The Arrhenius equation used for each sample size was as follows (Martin 1993), i.e.,

$$K = Ae^{-Ea/RT}$$

or $$\ln(K) = \ln(A) - \frac{Ea\ (1/T)}{2.303R}$$

where K = specific reaction rate (min^{-1})

A = Arrhenius factor

Ea = energy of activation (KJ/mol)

R = gas constant (8.314 J/Kmole)

T = absolute temperature (K)

By plotting 1/T against ln(K), the intercept on the vertical axis was ln$A$ and the slope of the line so obtained was –Ea/2.303R from which Ea may be obtained.

In the case of large particle, three data points of temperatures were fitted (Figures 21). This was the result of the compact of anhydrous form on the surface that protected the dehydration at higher temperature of each sample as discussed previously. The resulting activation energies (Ea) for dehydration vary with particle size: large particles (intact) have an Ea of approximately 178.45 KJ/mol, which is lower than those of medium and small crystals, of which the activation energy is 237.42 KJ/mol, and 239.44 KJ/mol, respectively (Table 9). In the case of small particle, the activation energy was calculated from its dehydration rate of the group at low temperature (below 85.5 °C).

Table 9 Activation energies of beclomethasone dipropionate monohydrate

Sample	Ea (KJ/mol)	Mechanism
Large size (intact)	178.45	Avrami-Erofeev (n = 1/3)
Medium size (ground)	237.42	Avrami-Erofeev (n = 1)
Small size (ground)	239.44	Avrami-Erofeev (n = 1)

Interestingly, the results show that the activation energies for dehydration increased with decreasing particle sizes. This is opposed to the most likely dehydration behavior of other compounds where there is a tendency that a lower activation energy is observed for smaller particle as reported in the dehydration of theophylline monohydrate (Agbada and York, 1994), trehalose dihydrate (Taylor and York, 1998), lactitol monohydrate (Yajima et al., 1997). Their result were due to the enhanced dehydration rate from the greater surface to mass/volume ratio of the smaller particles and the smaller particle expresses more lattice defects from grinding, enabling the water to be released more easily. Moreover, grinding produces an amorphous state, which affects bonding force between water-drug molecules and therefore facilitates water removal (Ito et al., 1996; Kitamura et al., 1989).

But in this study, it was found that Ea is higher in smaller particles (medium and small crystals) than the large particle (intact crystals). This could due to the grinding process that may initially produce the anhydrous portion on the surface of the particles, which acted as the shield (the surface barrier effect) against any future dehydration process. This shield hindered water removal of the crystal resulting in higher Ea needed for dehydration of the crystal as discussed above.

Besides, it is possible that higher water content within the particles generated a higher water vapor pressures inside the large particles during the heating process and

promoted the dehydration reaction (Landin et al., 1994). There was a similar report that, the total fraction releasablity of ethylene-vinyl acetate microspheres was found to increase as the volumetric loading and the excipients osmotic activity (sodium chloride, sodium carbonate) increased. The total fraction releases were enhanced by induction of polymer membrane rupture by osmotic pressure (Amsden and Cheng, 1994). As a result, the activation energy needed to dehydrate larger crystals is less than that needed for smaller crystals.

3.2 Structural stability (solid state stability) of hydrated beclomethasone dipropionate

The x-ray spectra of dehydrated beclomethasone dipropionate at various temperatures are shown in Figures 24, 25, and 26. From the previous study by Nachiengtung (1997), it was found that the interconversion of beclomethasone dipropionate was as follow:

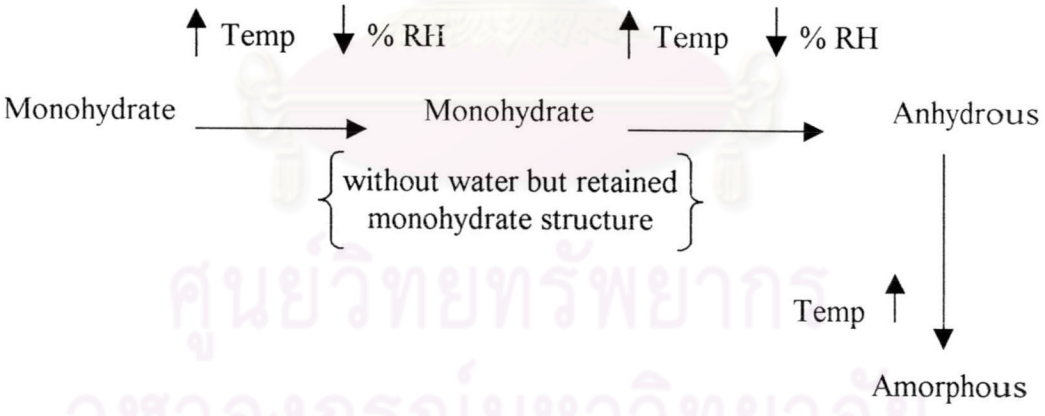

The x-ray powder diffraction analysis was used to measure the extent of structural changes until dehydration was completed (approximately 3.34% weight loss) when heated. Major peak positions used for marker were $2\theta = 8.303°$ and 18.485° for the monohydrate and anhydrous phases, respectively.

Unfortunately, in this study, the experimental results did not show a correlation of time at which complete dehydration occurred between TGA study and x-ray powder analysis. A complete dehydration of hydrate form was done in the convection oven. It might be due to the samples in the oven had higher thickness and limited surface area for dehydration. Hence, the time for complete dehydration in the oven was longer than the time obtained by TGA. However, the x-ray spectra were determined immediately after the dehydration level at various temperatures had reached approximately 80-90% (Appendix E). X-ray spectra of each sample showed the gradual structural change from crystalline monohydrate to a mixture of anhydrous and hydrated phase and eventually to pure anhydrous compound. This result was in accordance with Nachiengtung (1997) in regard that the structure of crystal was still monohydrate form after a complete dehydration (without water but retained monohydrated structure).

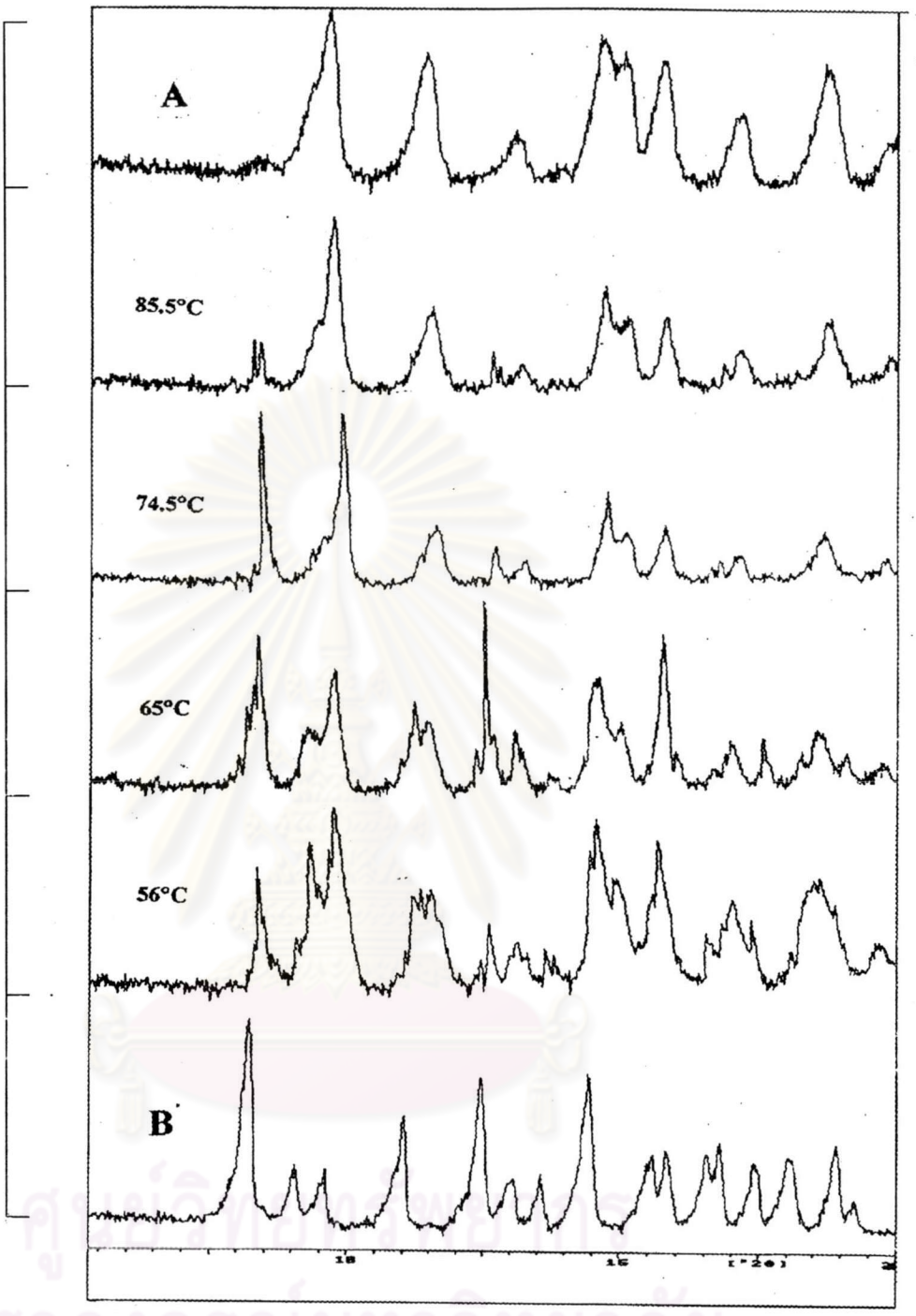

Figure 24 X-ray spectra of dehydrated beclomethasone dipropionate of large particle (intact crystals) at various temperatures and times. (85.5°C/ 50 min, 74.5°C/120 min, 65°C/240 min, 56 °C/750 min; as compared with (A) anhydrous form and (B) monohydrate form)

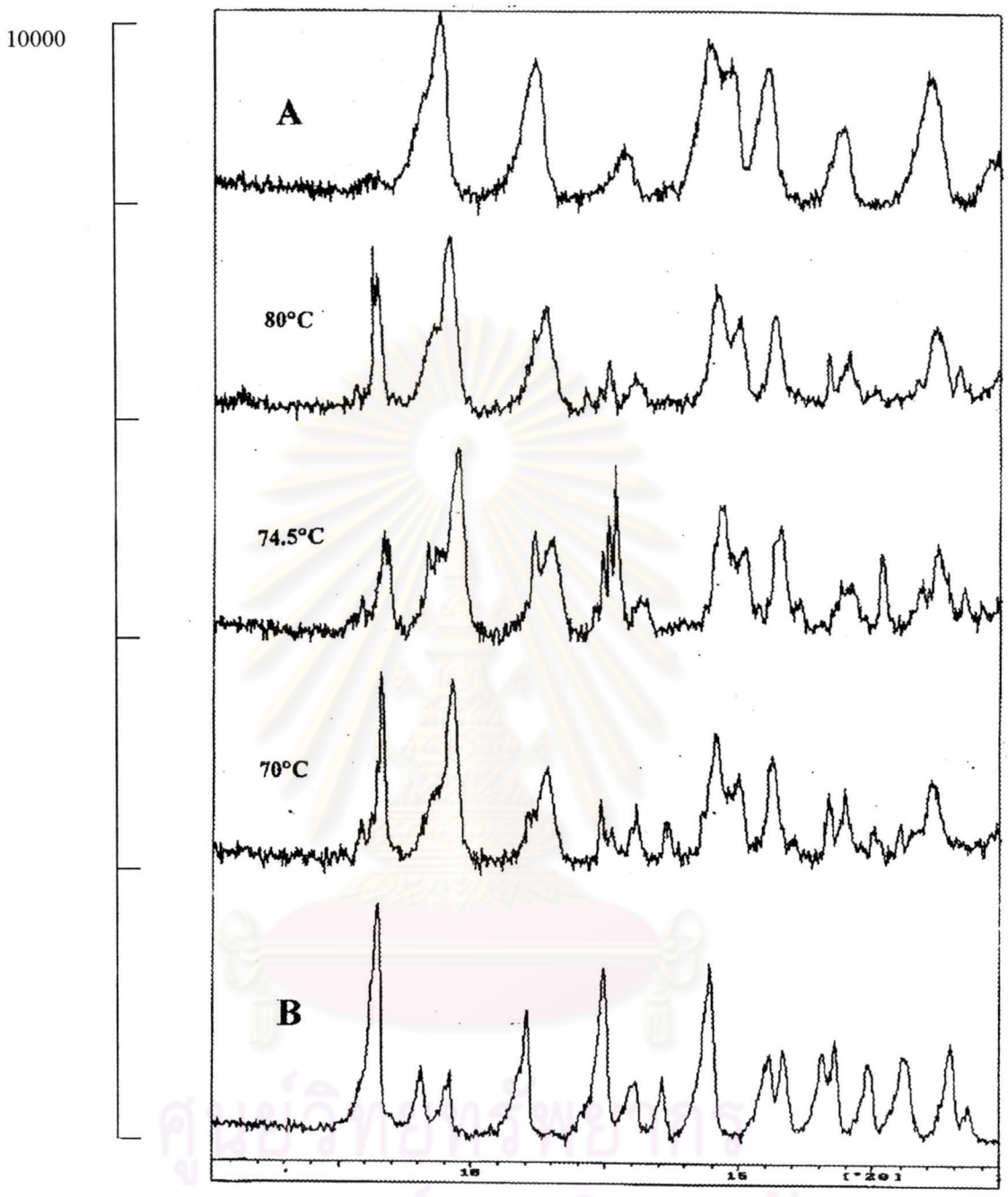

Figure 25 X-ray spectra of dehydrated beclomethasone dipropionate of medium particles at various temperatures and times. (80°C/150 min, 74.5°C/250 min, 70 °C/330 min; as compared with (A) anhydrous form and (B) monohydrate form)

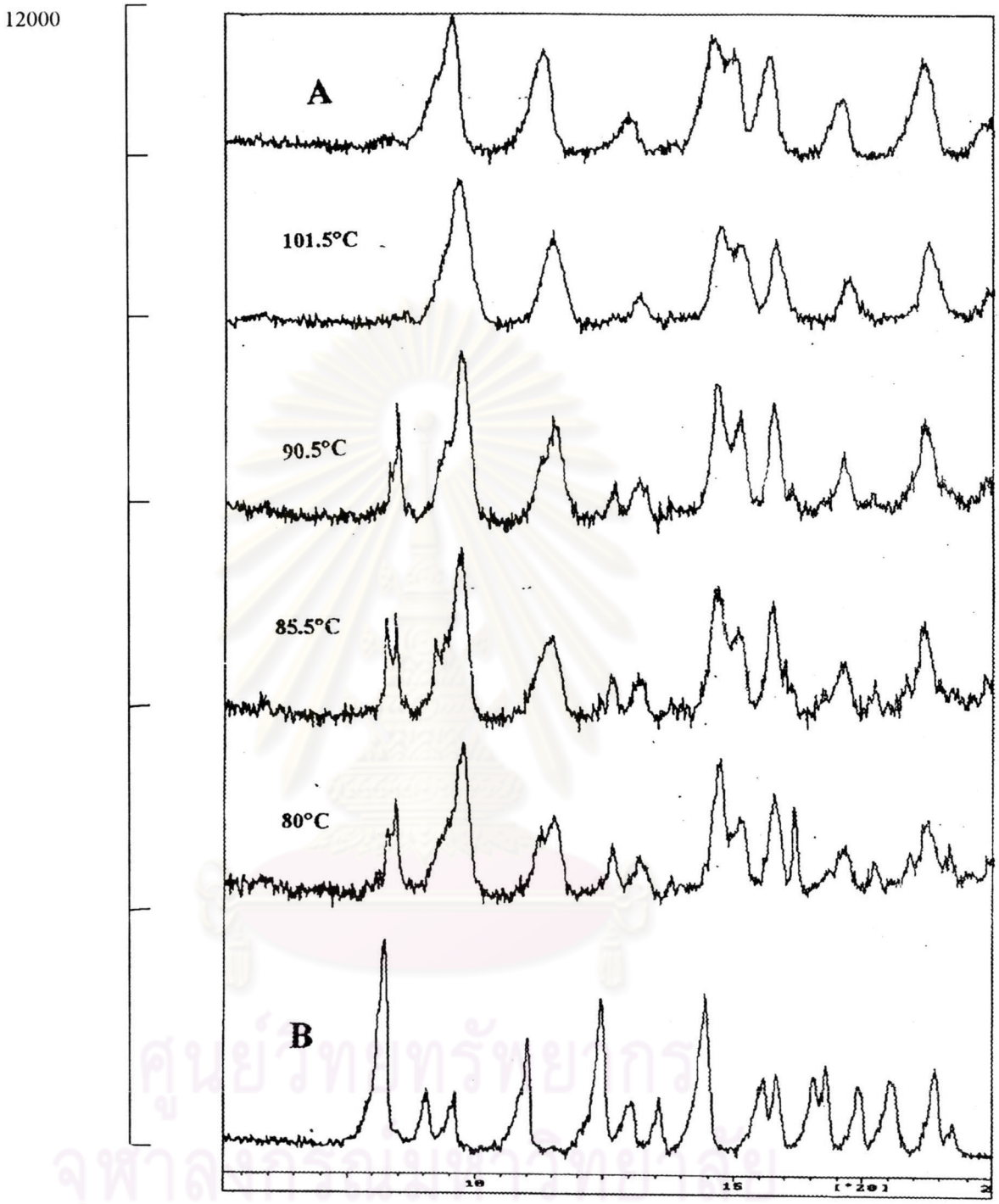

Figure 26 X-ray spectra of dehydrated beclomethasone dipropionate of small particles at various temperatures and times. (101.5°C/75 min, 90.5°C/180 min, 85.5°C/210 min, 80 °C/300 min; as compared with (A) anhydrous form and (B) monohydrate form)

Nevertheless, phase change patterns obtained from all samples indicated that the trend for transformation to anhydrous phase is greater at higher temperatures as indicated by the position $2\theta = 18.485°$ for anhydrous form and position $2\theta = 8.303°$ for monohydrated form. At the highest temperature applied to the three samples, peak position of anhydrous form of beclomethasone dipropionate was prominent while the position peak of monohydrate was less intense. These results are supportive of the result of the isothermal TGA where the dehydration rates at higher temperatures were altered by a compact anhydrous layer generated on the surface of particles during dehydration process. In the case of small particles where two mechanisms of dehydration were assumed, it was possible that the anhydrous phase transformed to a metastable phase or amorphous state at high temperatures (101.5 and 90.5 °C). This assumption was confirmed by the work of Nacheingtung (1997) that beclomethasone dipropionate when heated will transform eventually to an amorphous solid. The amorphous state generated on the surface was so minute (approximately less than 10%w/w), x-ray powder diffractometer could not determine its existence. However, the amount of amorphous phase was just enough to increase the rate of dehydration. This higher energetic state of amorphous phase resulted in a decrease in physical and chemical stability, thus these high temperatures should not be used in size reduction.

The solvent stability could be determined by weight loss during the dehydration process (Leung et al., 1998). Dehydration of beclomethasone dipropionate monohydrate seems to result in anhydrous form. Phase transformation occurs only after the water is removed from the crystal lattice. TGA and kinetics of desolvation indirectly describe solvent stability within the crystal lattice. Thus the solvent stability of samples was concluded as large particle (intact) < medium and small particle (temperature lower than 85.5°C).

3.3 Particle size determination after dehydration

3.3.1 Laser light scattering was used in this experiment to determine the particle size of beclomethasone dipropionate monohydrate before and after dehydration.

The monohydrate samples obtained from Section 3.2 were subjected to dehydration process. Tables 10, 11 and 12 show the particle sizes of large particles (intact crystal), medium particles and small particles after dehydration process at various temperatures. All samples were immediately analyzed after completely dehydrated (approximately 3.34% water loss).

Table 10 Changes in particle size of large particles (intact crystals)

Temperature (°C)	d(v,0.1) (SD) μm	d(v,0.5) (SD) μm	d(v,0.9) (SD) μm
(Before dehydration)	213.93 (8.50)	429.89 (10.97)	758.79 (18.13)
85.5	13.70 (0.70)	48.10 (1.58)	131.23 (3.15)
74.5	20.36 (0.13)	58.34 (0.66)	120.34 (3.44)
65.0	34.57 (2.25)	112.31 (0.64)	226.29 (5.66)
56.0	134.57 (2.06)	311.54 (2.91)	665.86 (15.12)

Table 11 Changes in particle size of medium particles

Temperature (°C)	d(v,0.1) (SD) μm	d(v,0.5) (SD) μm	d(v,0.9) (SD) μm
(Before dehydration)	83.80 (0.32)	150.80 (0.42)	259.39 (0.81)
80.0	10.73 (0.12)	42.78 (0.12)	96.73 (2.05)
74.5	15.32 (0.43)	45.39 (0.76)	112.93 (2.00)
70.0	13.77 (0.24)	46.68 (0.31)	112.83 (5.14)

Table 12 Changes in particle size of small particles

Temperature (°C)	d(v,0.1) (SD) μm	d(v,0.5) (SD) μm	d(v,0.9) (SD) μm
(Before dehydration)	4.24 (2.83)	63.88 (11.25)	123.13 (7.32)
101.5	8.81 (0.26)	36.41 (0.35)	73.29 (0.54)
90.5	15.54 (0.77)	46.82 (0.60)	101.34 (0.60)
85.5	17.93 (1.06)	47.78 (1.12)	95.66 (2.14)
80.0	16.19 (0.64)	46.81 (0.77)	96.47 (1.35)

The particle size in these samples were compared using the median of particles d(v,0.5) as shown in Tables 10, 11, and 12. The data shows mainly unimodal dispersion with minor tailing to the left side with the total of less than 5% as seen in Figure 27. Particle sizes from SEM photomicrographs of all three samples were reduced as shown in Figure 28, expect with the small particles, having the particle size very similar to the original particle when dehydrated at 101.5°C. This was probably due to the agglomeration of fine particles on the surface of a larger particle after dehydration. This is clearly shown in Figure 29. Laser light scattering method, however, (Table 12) actually demonstrated there was a reduction of particles from the median of 63.88 to 36.41 μm since the suspending agent disperses the agglomerated particles.

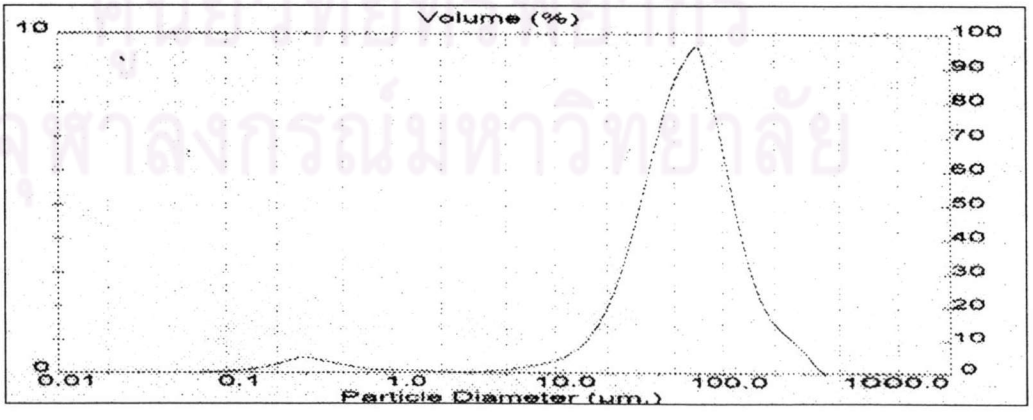

Figure 27 An example of size distribution curve of dehydrated intact crystals at 85.5 °C

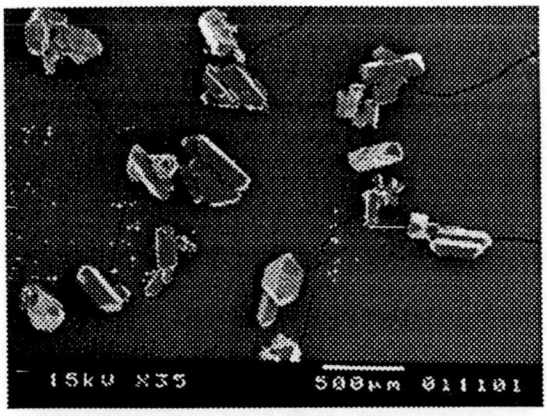

A1) large crystals before dehydration

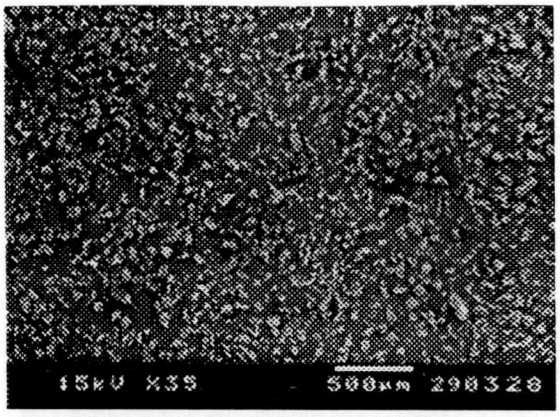

A2) after dehydration at 85.5 °C

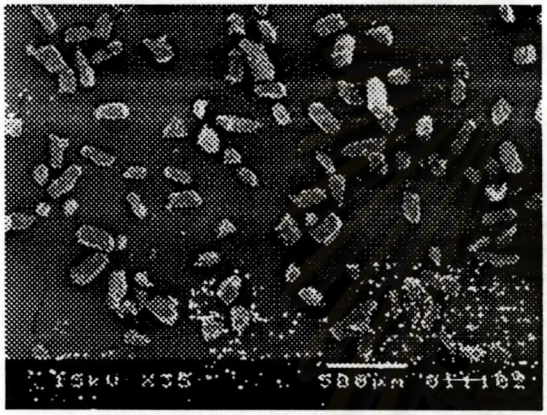

B1) medium crystals before dehydration

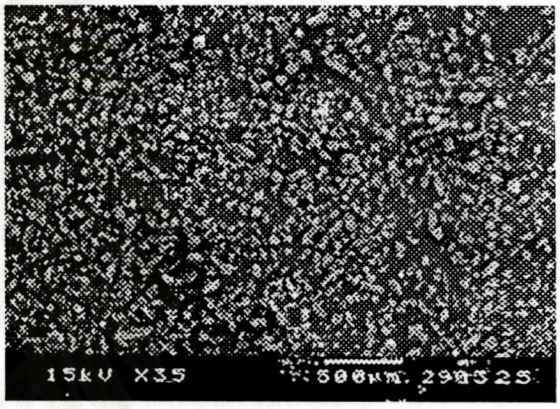

B2) after dehydration at 80°C

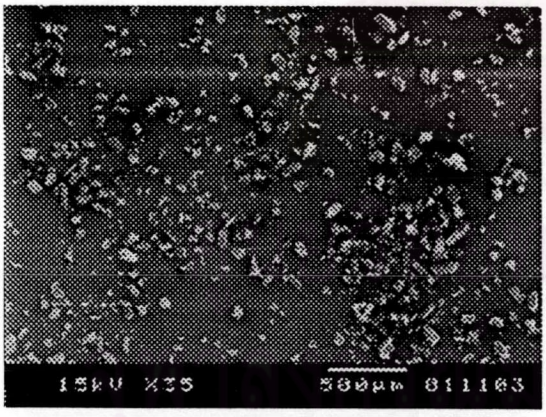

C1) small crystals before dehydration

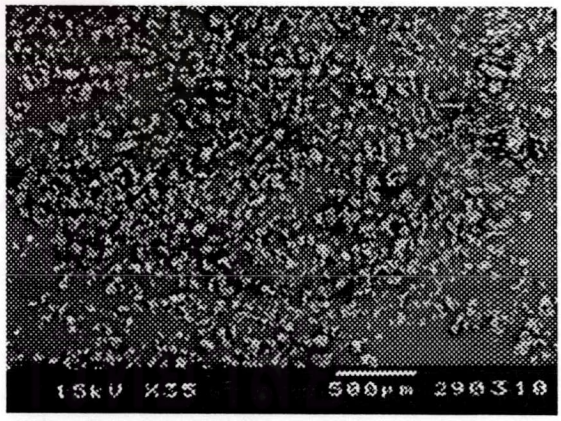

C2) after dehydration at 101.5 °C

Figure 28 SEM of hydrated beclomethasone dipropionate before and after dehydration (35 × magnification)

Effect of original size of the particle. With regards to ground samples (medium and small particles), the median of particle sizes when various temperatures

were used to dehydrate indicated that there were no significant difference among the sizes of particles obtained from dehydration at different temperature. ($p>0.05$) (Appendix F). The electronphotomicrograph (Figure 29) shows that the medium and small crystals collapse to irregular shape as the same size. However, the product of small crystal has a very porous structure with agglomerated fine particles on the surface. It is expected that the size reduction might be limited by the unit cell of crystal, that is, the reduction of particles ceased when it was equal to its unit cell.

Although the original size of the particle did not play a role in the resulting size of the particles after desolvation but it had a significant influence on the rate of dehydration. At the same temperature treated (80.0 °C), the rate constant (k) of dehydration in larger crystals is higher than that of smaller crystals (0.0988 min^{-1} for medium versus 0.0434 min^{-1} for small crystals) from Tables 7 and 8, respectively. This could due to the influence of higher water vapor pressure in larger particles as previously discussed.

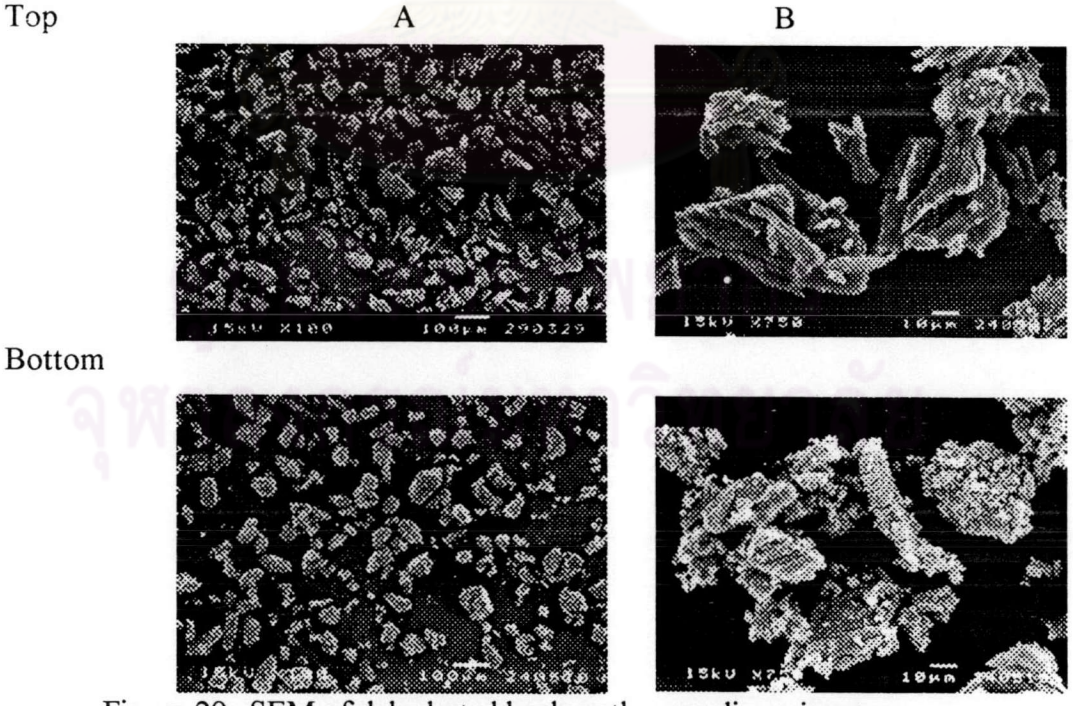

Figure 29 SEM of dehydrated beclomethasone dipropionate
Top: medium crystal at 80 °C; Bottom: small crystals at 101.5 °C.
A. 100× magnification B. 750× magnification

Effect of temperature. For ground samples (medium and small particles), temperature has no impact on the size after dehydration, i.e., any temperature applied resulted in similar size reduction (Tables 11 and 12). However, in intact crystals (large particles), the particle size reduction was obvious only when the temperature was above 65.0 °C (Table 10). As the temperature rise, the structure underwent significant reduction in particle size, collapsed and fractured as shown in Figures 30A and 30B.

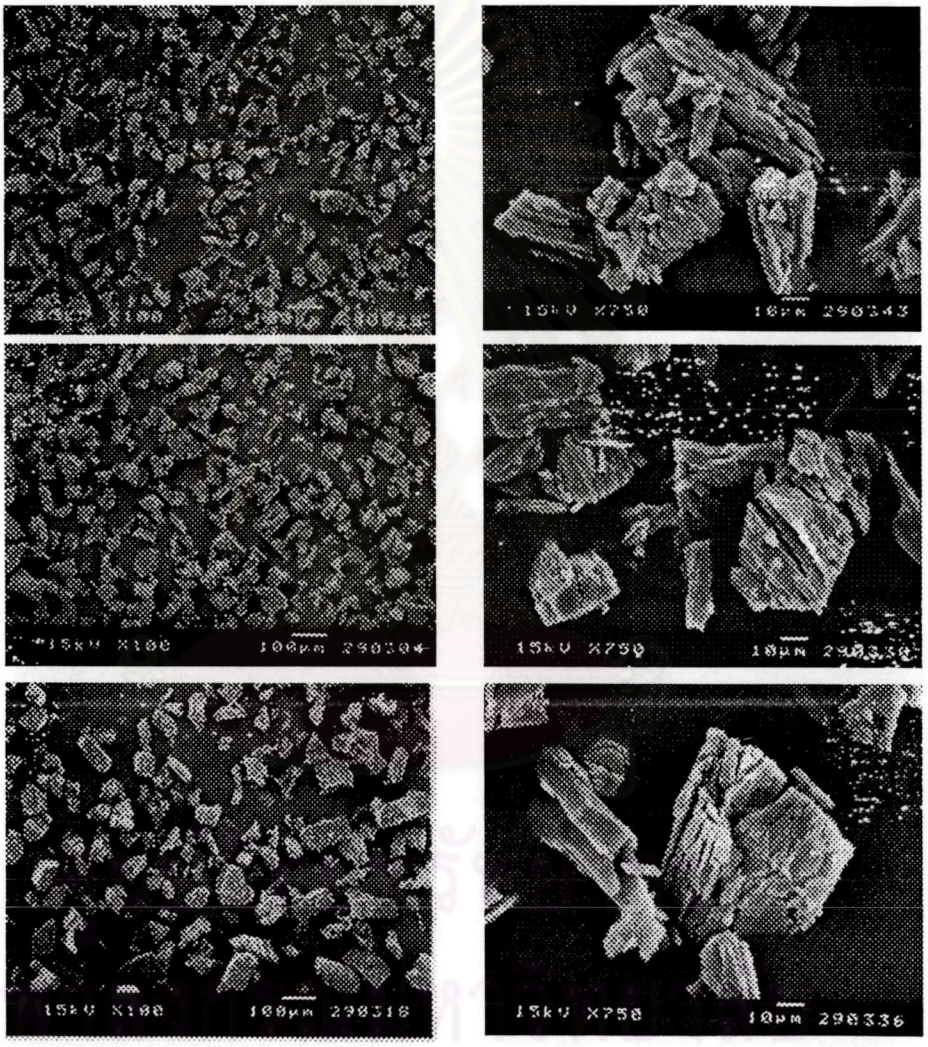

Figure 30A SEM of large crystals of dehydrated beclomethasone dipropionate
Top: 85.5 °C; Middle: 74.5 °C; Bottom: 65 °C
Left: 100× magnification. Right 750× magnification.

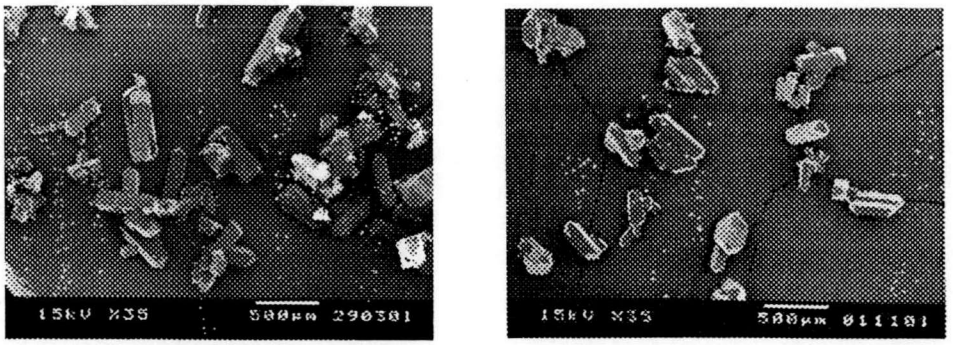

Figure 30B SEM of large crystals of dehydrated beclomethasone dipropionate Left: 56°C, Right: Before dehydration, 35× magnification

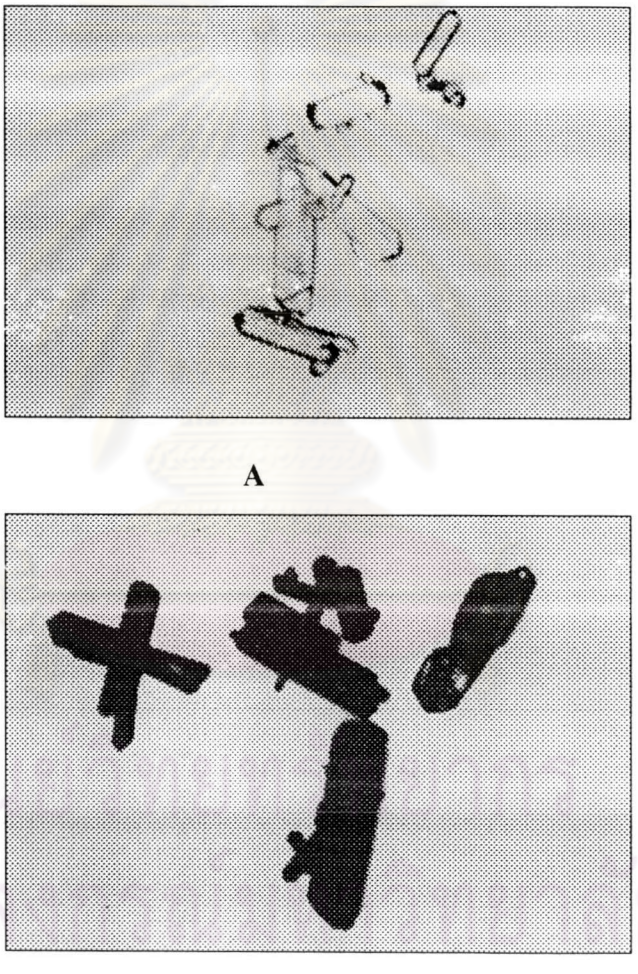

A

B

Figure 31 The photograph of large crystals of dehydrated beclomethasone dipropionate at 56 °C A) before dehydration, B) after dehydration

In contrast, large crystals did not collapse at 56 °C, but only appeared opaque as observed by light microscope (Figure 31). This is in accordance with Clay et al. (1982) and Byrn et al. (1999) of an event occurred after dehydration.

Therefore, particle size reduction of large particle (intact) was largely dependent upon the temperature used. The same possibility probably applied to the ground samples (medium and small size) except that the temperatures used to dehydrate these samples were higher than 65°C, thus, the temperature dependent particle size reduction was not observed.

The x-ray structures show that after dehydration the structures were prone to rearrange from monohydrate to anhydrous form with the structure collapse to fine particle in all three sizes. However, low temperature (56°C) could only resulted in the removal of water and structural rearrangement as seen the large particles but not a fully collapsed particle. But after heating the particles for another 72 hours, it showed that particles collapsed to certain size (approximately 40 μm). Thus the result in particle size reduction depends upon both the rate of dehydration of water molecules from the lattice and the rearrangement to anhydrous form when introduced with sufficient heat energy to facilitate the collapse of particles.

3.3.2 BET method was employed to determine specific surface area of the crystals before and after dehydration. The results are shown in Tables 13 and 14, respectively.

Table 13 Specific surface area of the crystals before dehydration of the samples

Sample	Specific surface area (m^2/g) before dehydration
Large particles (intact)	0.387
Medium particles	0.262
Small particles	0.249

The results in Table 13 did not follow the fact that the larger particles should have small specific surface area. This was due to the fact that in this study, nitrogen gas could not be fully adsorbed onto the surface of the particles because water removal process of BET technique using 100°C temperature would highly interfered with the physicochemical characteristics of the particle of interest, and hence, the dehydration process.

Table 14 Specific surface area of the crystals after dehydration of the samples

Sample	Temperature at dehydration	Specific surface area (m^2/g) after dehydration
Large particles (intact)	85.5 °C 74.5 °C 65.0 °C 56.0 °C	1.423 1.450 1.658 0.489
Medium particles	80.0 °C 74.5 °C 70.0 °C	1.494 1.504 1.173
Small particles	101.5 °C 90.5 °C 85.5 °C 80.0 °C	1.532 1.235 1.175 1.751

In contrast to Table 13, particles in Table 14 were dehydrated. Moisture contents were properly removed from the particles and as a result, nitrogen gas was fully adsorbed onto the surface of the particles. BET method revealed that dehydrated form had higher specific surface area than the monohydrate form. In terms of reliability, figures in Table 14 roughly report the specific surface areas of different particle sizes at generated from different temperatures. Besides, each sample underwent single measurement. Therefore, the result in Table 14 partially supported the particle size analysis described in the previous section. Of note, specific surface area of large particles at 56.0 °C (0.489 m^2/g) confirmed the occurrence that crystals did not collapse at this temperature.